Results from the BES program at STAR

Hanna Zbroszczyk for the STAR Collaboration

hanna.zbroszczyk@pw.edu.pl

Warsaw University of Technology

Supported in part by

U.S. DEPARTMENT OF ENERGY

NATIONAL SCIENCE CENTRE POLAND

EXCELLENCE INITIATIVE RESEARCH UNIVERSITY

Outline

- Beam Energy Scan Program
- QCD phase diagram
- Experiments
- Main questions
- Summary and perspectives

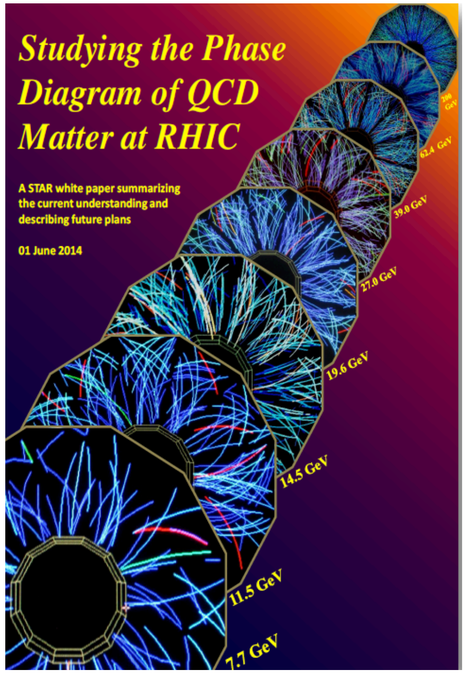

http://drupal.star.bnl.gov/STAR/starnotes/public/sn0598

Outline

- Beam Energy Scan Program
- QCD phase diagram
- Experiments
- **Main questions**
- Summary and perspectives

Goals of the Beam Energy Scan Program:

1. Search for **turn-off** of **QGP** signatures
2. Search for signals of the **first-order phase transition**
3. Search for QCD **critical point**
4. Search for signals of **Chiral symmetry restoration**

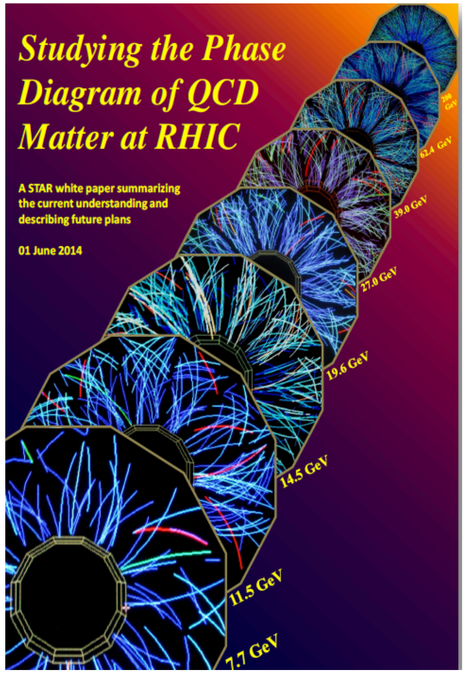

http://drupal.star.bnl.gov/STAR/starnotes/public/sn0598

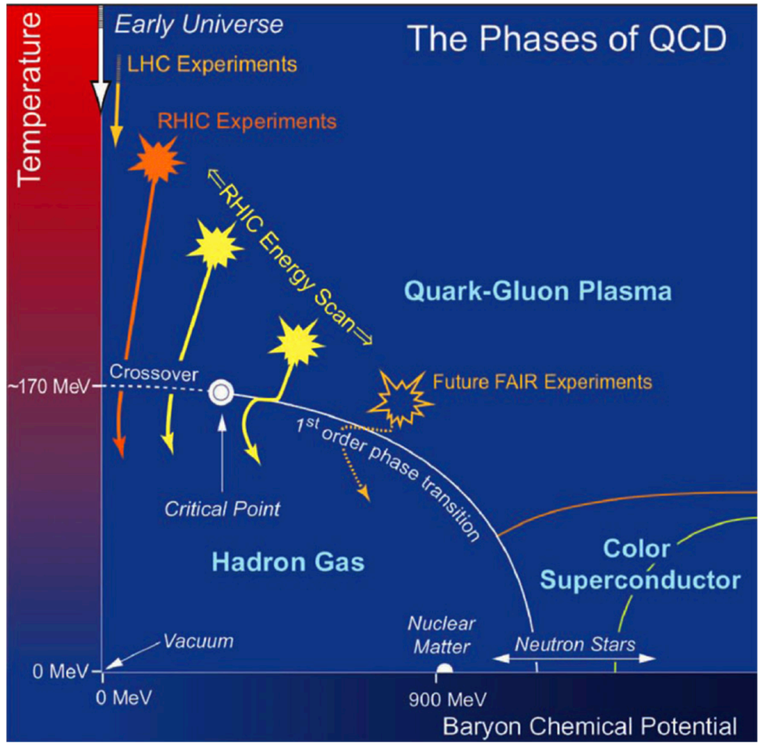

Probing QCD Phase Diagram with Heavy-ion collisions

Heavy-ion collision used as a tool to probe QCD phase diagram

Believed to be understood:

Lattice QCD predicts a smooth **cross-over** transition at large T and $\mu_B \sim 0$

Various models predict **first-order phase transition** at large μ_B

Critical point is believed to exist, but.. where?

Strategy: to map the phase diagram (μ_B ,T) using heavy-ion collisions changing their collision energy: BES-I, BES-II (+FXT)

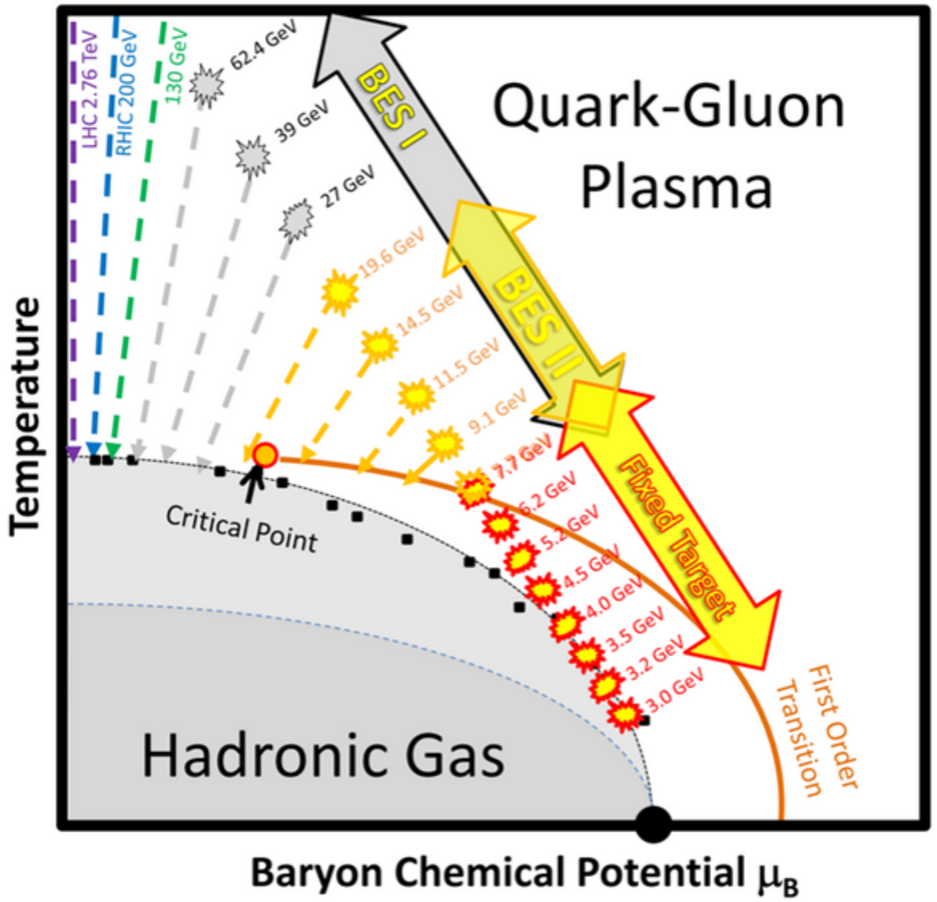

STAR detector system

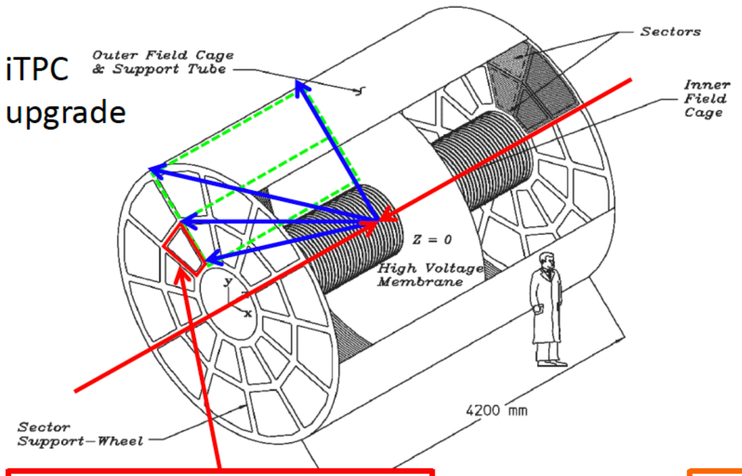

TPC inner sector readout with more segmentation

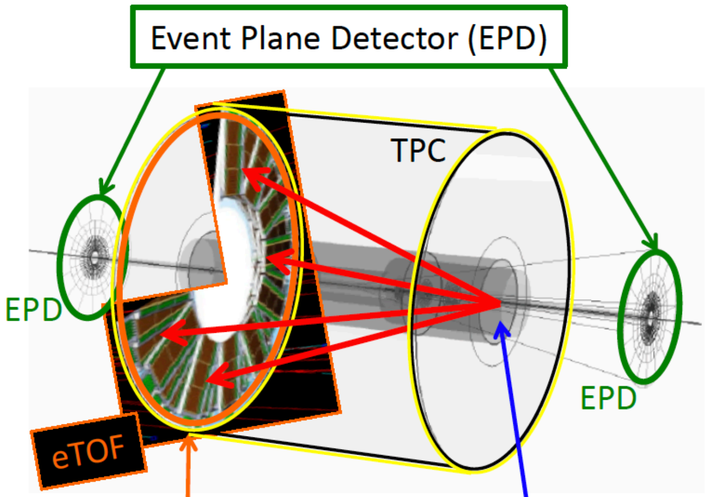

End-cap Time-of-Flight (eTOF) from FAIR-CBM

Fixed target mode

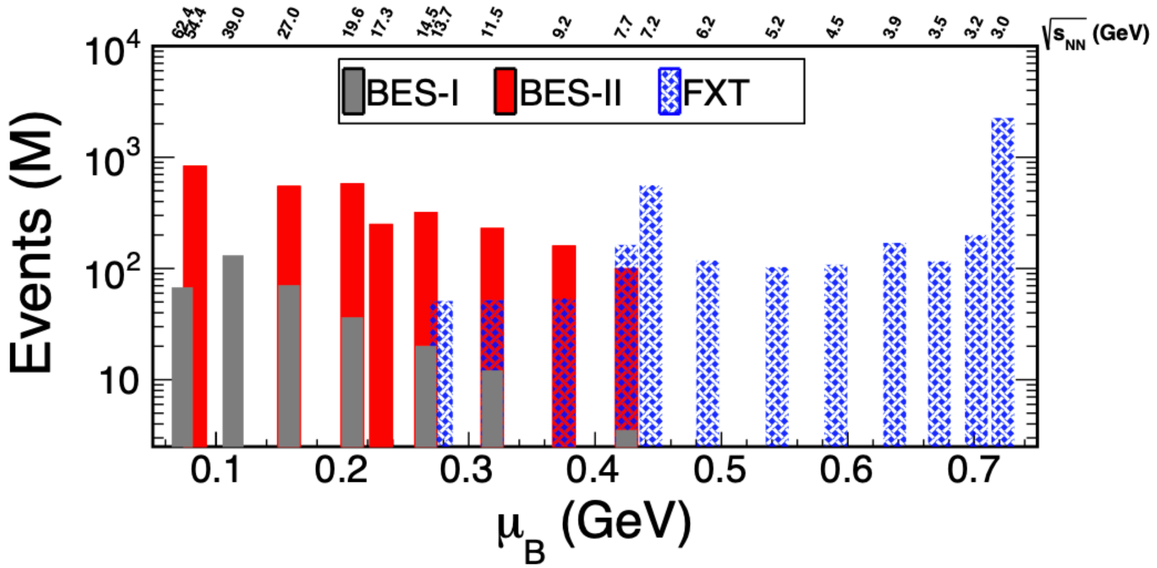

Solenoidal **T**racker **A**t **R**HIC originally designed to search for **Quark Gluon Plasma**.

BES program started at 2010.

Luminosity of the RHIC collider-mode is unusable for $\sqrt{s_{NN}} < 7.7$ GeV.

Fixed-target (FXT) program extends the collision energy and μ_B coverage.

Particle spectra

PHYSICAL REVIEW C **101**, 024905 (2020)

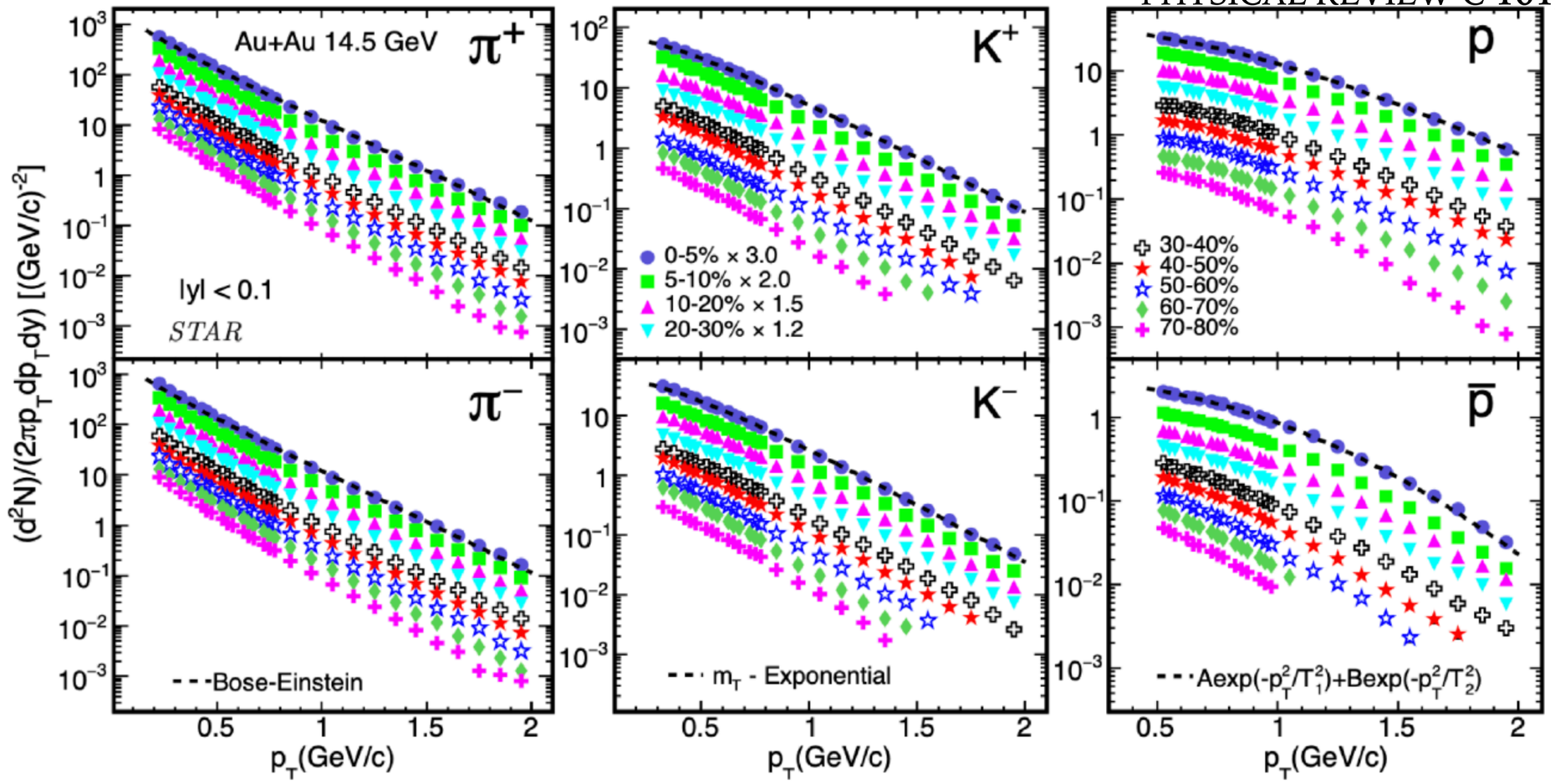

Inverse slopes of the identified hadron spectra follow the order π < K < p

$$\frac{dN}{m_T dm_T dy} = f(y) exp(\frac{-m_T}{T}); m_T = \sqrt{m^2 + p_T^2}$$

Chemical and kinetic freeze-out parameters

PRC 96 (2017) 4, 044904

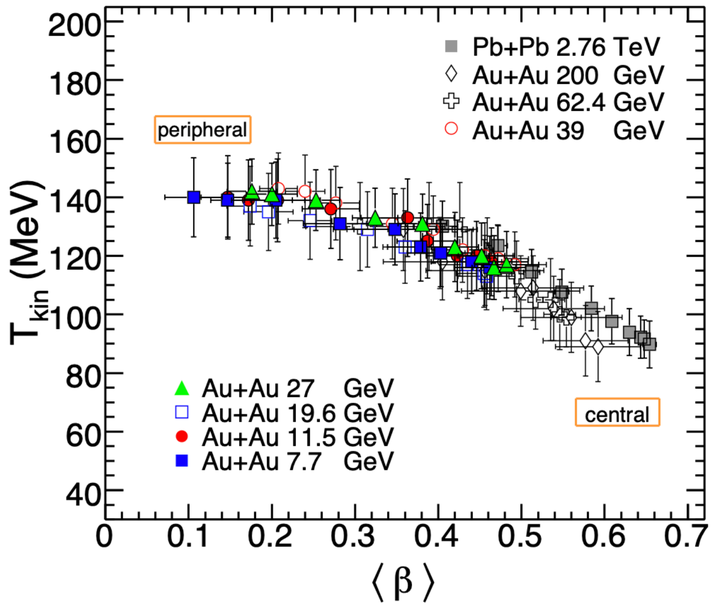

Extracted from spectra:

$m_T - m$ of π, K, p

Chemical and kinetic freeze-out parameters

PRC 96 (2017) 4, 044904

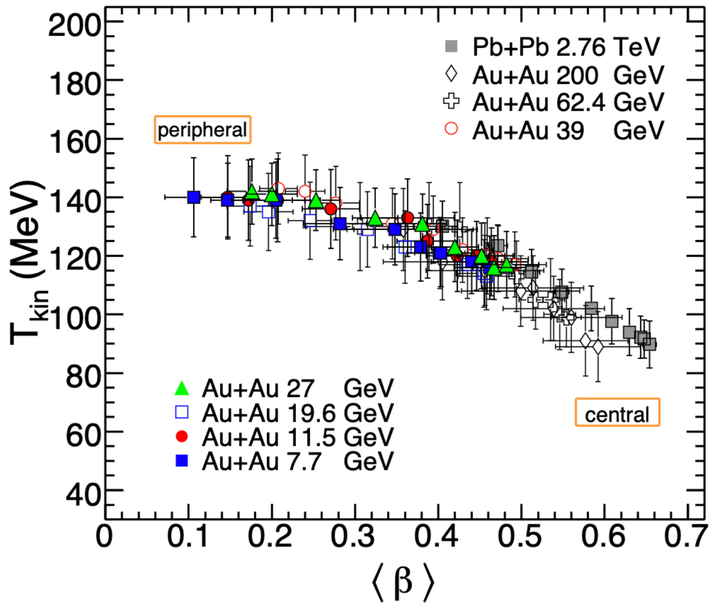

Extracted from spectra (from Blast Wave model):

$m_T - m$ of π, K, p

Extracted from particle yields with THERMUS model

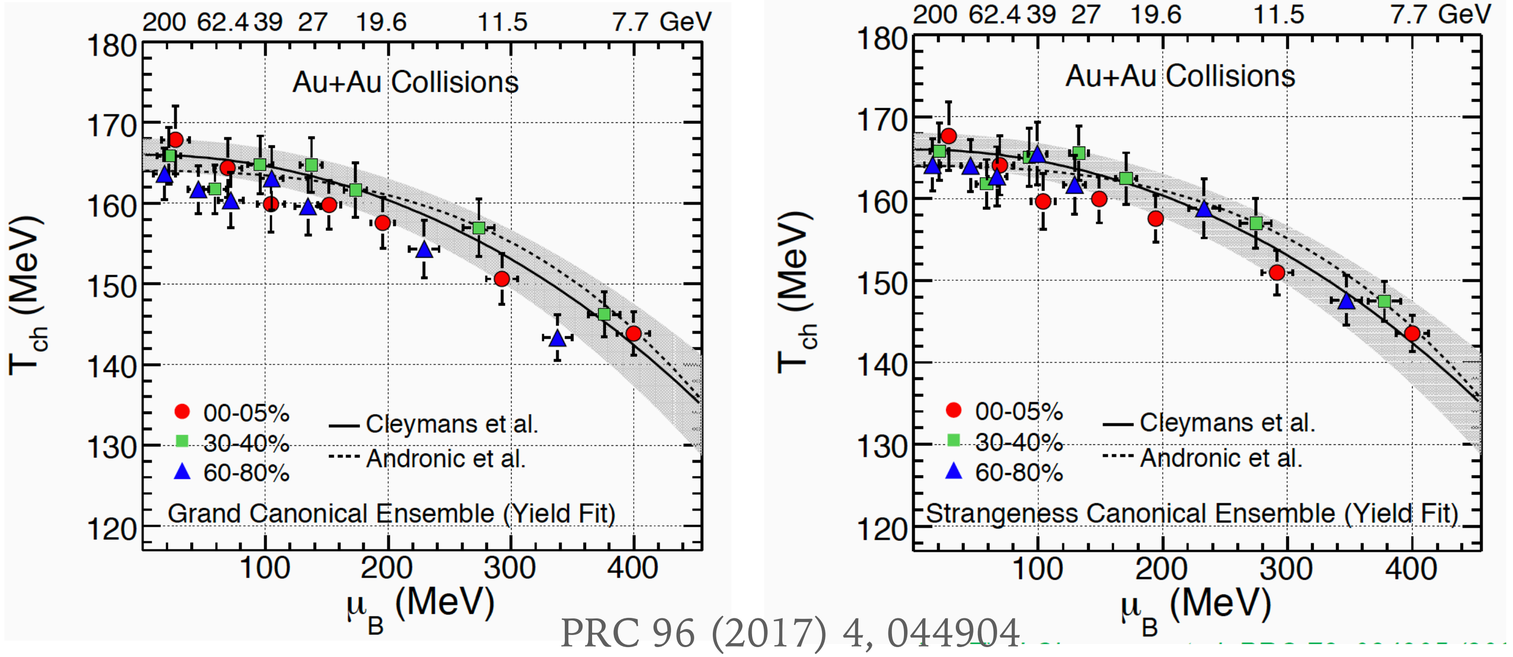

PRC 96 (2017) 4, 044904

Extracted from particle yields with THERMUS model assuming Grand (Strangeness) Canonical ensemble.

BES-I: $\mu_B \sim 20$ MeV - 420 MeV

BES-II: $\mu_B \sim 205$ MeV - 720 MeV

Observables

1. **Onset of QGP** (disappearance of signals of partonic degrees of freedom)

Charge separation w.r.t. EP

NCQ scaling of elliptic flow

2. Observation of **phase transition** (softening of EOS at lower collision energy)

Directed flow v_1

Femtoscopy

3. Existence of **Critical Point** (CP)

Fluctuation analyses

4. **Chiral symmetry restoration**

Low-mass vector mesons, dileptons CME

5. … and **beyond ..**

Light nuclei

Lambda's polarization

Hypernuclei production

Nuclear modification factor

Observables

1. **Onset of QGP** (disappearance of signals of partonic degrees of freedom)

Charge separation w.r.t. EP

NCQ scaling of elliptic flow

2. Observation of **phase transition** (softening of EOS at lower collision energy)

Directed flow v_1

Femtoscopy

3. Existence of **Critical Point** (CP)

Fluctuation analyses

4. **Chiral symmetry restoration**

Low-mass vector mesons, dileptons CME

5. … and **beyond ..**

Light nuclei

Lambda's polarization

Hypernuclei production

Nuclear modification factor

Charge separation

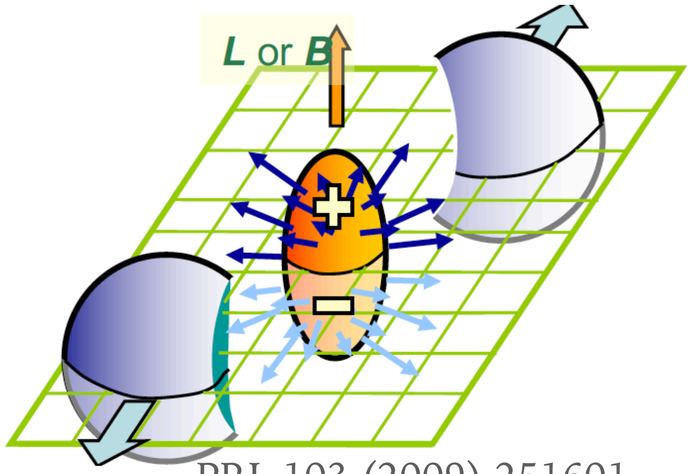

PRL 103 (2009) 251601

- Strong **B**, system is **deconfinement**, chiral symmetry restoration is reached.
- Chiral symmetry breaking and the origin of hadrons masses related to the existence of gluons field.
- Quarks interactions with gluons fields can change quarks chirality, and may lead to **L**ocal **P**arity **V**iolation.
- **C**hiral **M**agnetic **E**ffect: separation of the charges along the **B** axis (or **L**).

Charge separation

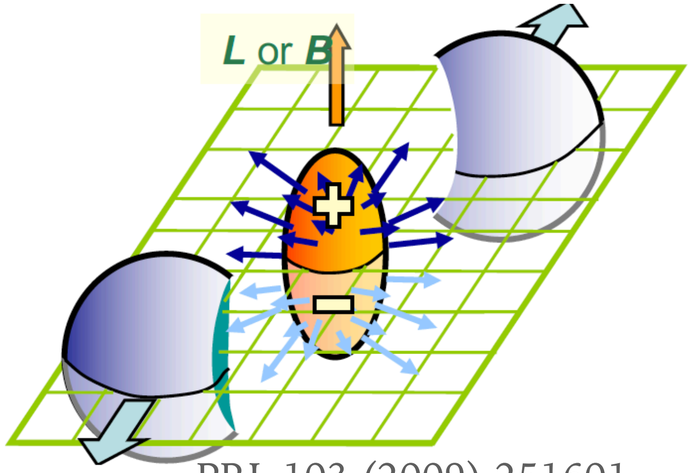

PRL 103 (2009) 251601

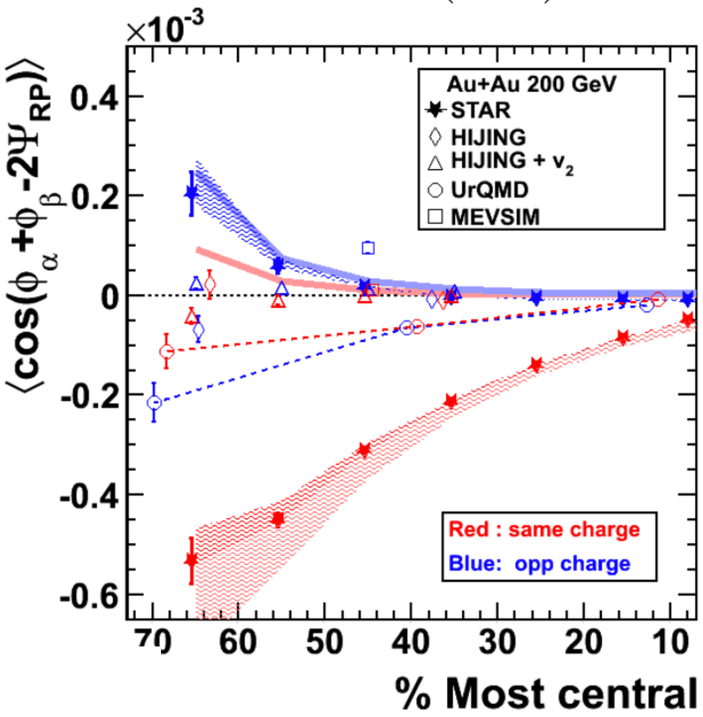

- Strong **B**, system is **deconfinement**, chiral symmetry restoration is reached.
- Chiral symmetry breaking and the origin of hadrons masses related to the existence of gluons field.
- Quarks interactions with gluons fields can change quarks chirality, and may lead to **L**ocal **P**arity **V**iolation.
- **C**hiral **M**agnetic **E**ffect: separation of the charges along the **B** axis (or **L**).

- Au+Au, U+U and Cu+Cu at top RHIC energies show charge separation measures as $\gamma = < cos(\phi_\alpha + \phi_\beta - 2\Psi_{RP}) >$

Charge separation

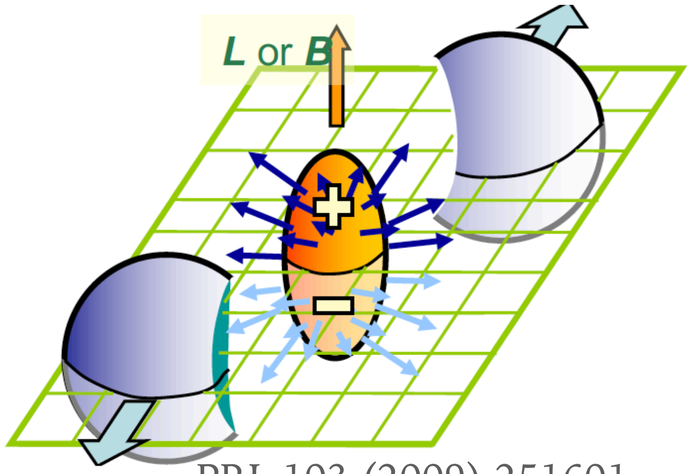

PRL 103 (2009) 251601

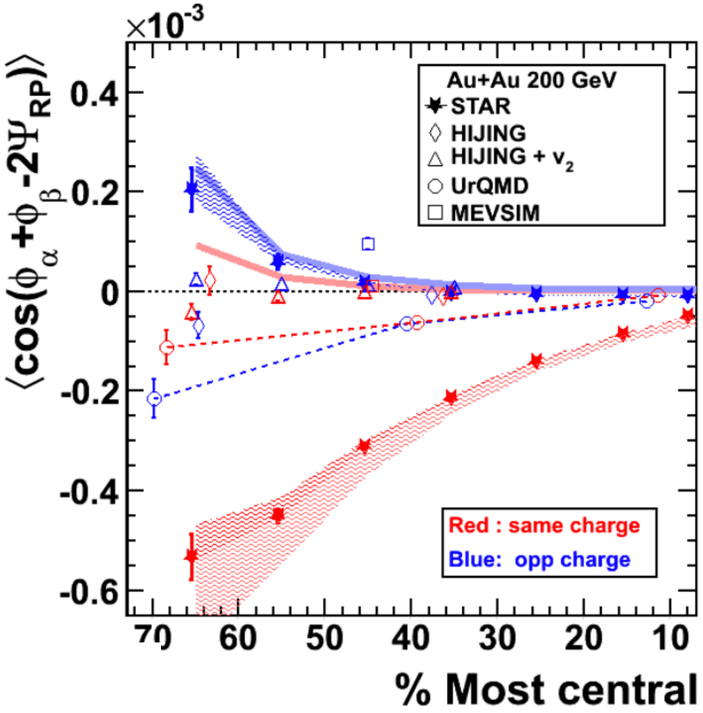

- Strong **B**, system is **deconfinement**, chiral symmetry restoration is reached.
- Chiral symmetry breaking and the origin of hadrons masses related to the existence of gluons field.
- Quarks interactions with gluons fields can change quarks chirality, and may lead to **L**ocal **P**arity **V**iolation.
- **C**hiral **M**agnetic **E**ffect: separation of the charges along the **B** axis (or **L**).

- Au+Au, U+U and Cu+Cu at top RHIC energies show charge separation measures as $\gamma = < cos(\phi_\alpha + \phi_\beta - 2\Psi_{RP}) >$

- Is reduction of signal with decreasing collision energy the signal of turn-off of deconfinement?

PRL 113 (2014) 52302

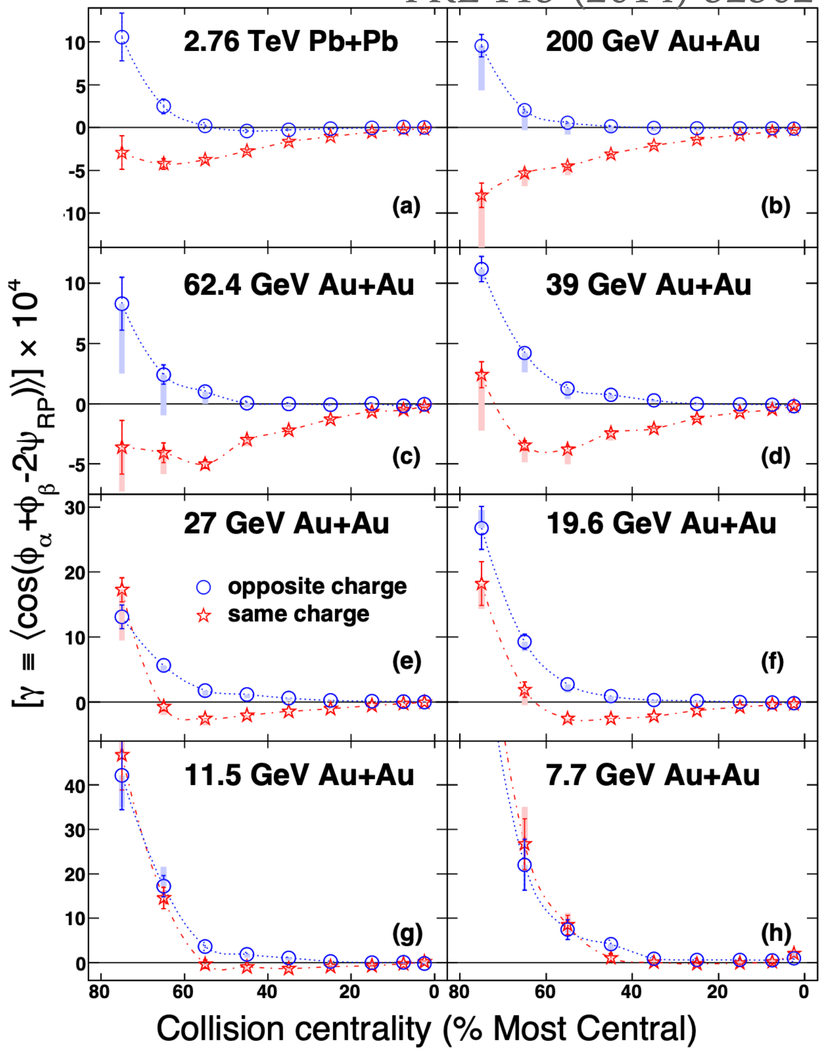

Splitting between same- and opposite-sign charges decreases with decreasing collision energy and disappears below $\sqrt{s_{NN}} = 11.5$ GeV

Elliptic flow

Initial spatial anisotropy leads to the final momentum anisotropy

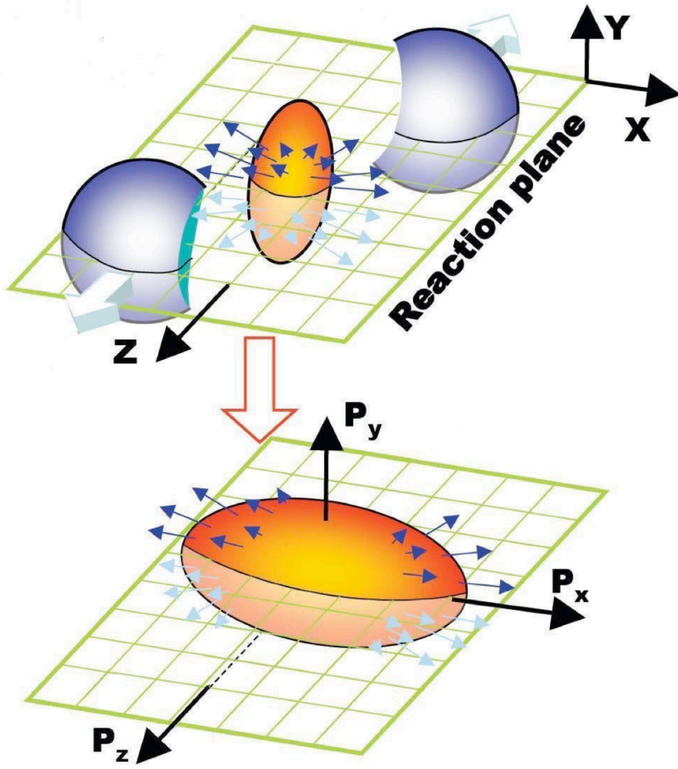

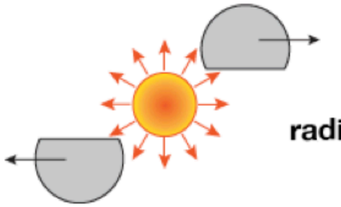

radial flow

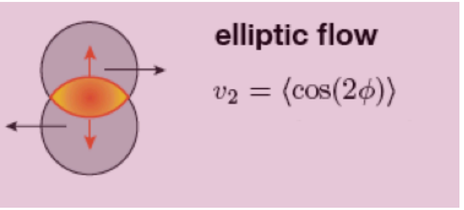

elliptic flow

$v_2 = \langle \cos(2\phi) \rangle$

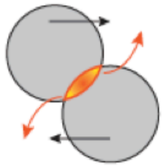

directed flow

$v_1 = \langle \cos(\phi) \rangle$

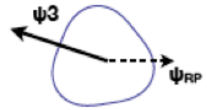

triangular flow

$v_3 = \langle cos(3\phi) \rangle$

$\phi = (\varphi - \Psi_{RP})$

$$E\frac{\mathrm{d}^3N}{\mathrm{d}^3\mathbf{p}} = \frac{1}{2\pi}\frac{\mathrm{d}^2N}{p_\mathrm{t}\mathrm{d}p_\mathrm{t}\mathrm{d}y}\left(1+2\sum_{n=1}^{\infty}v_n\cos[n(\varphi-\Psi_\mathrm{RP})]\right)$$

Elliptic flow

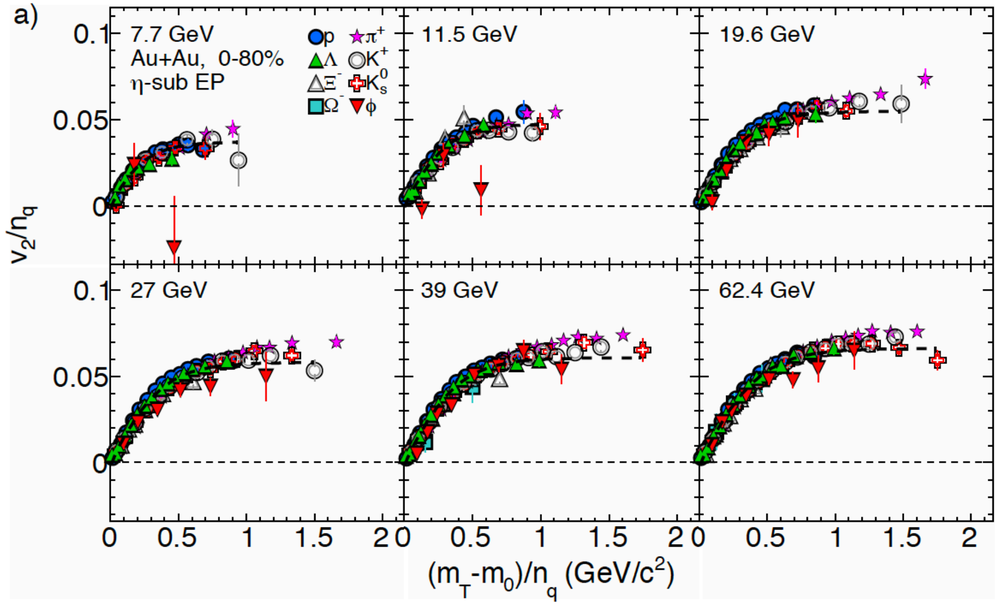

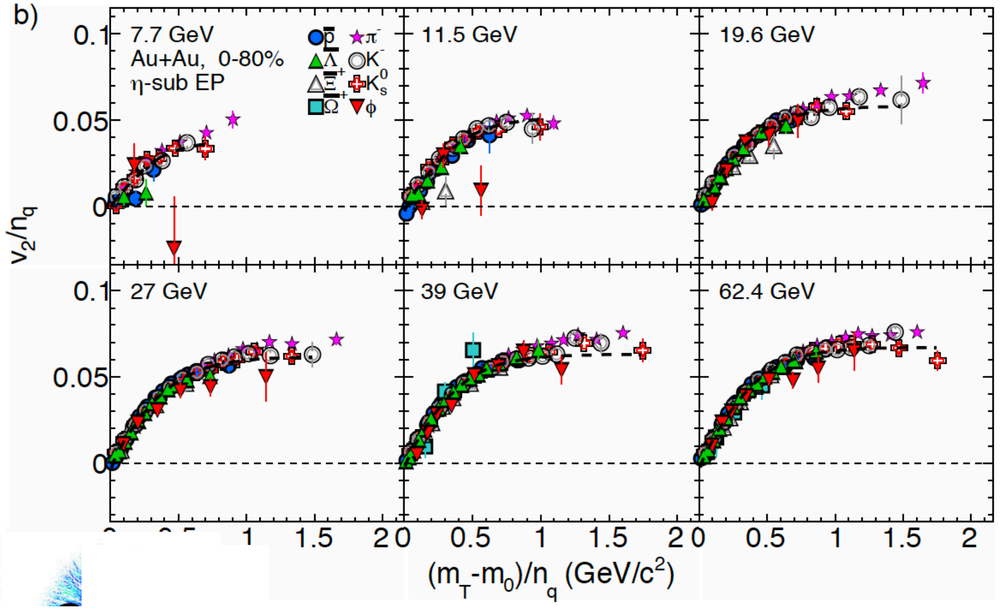

Initial spatial anisotropy leads to the final momentum anisotropy

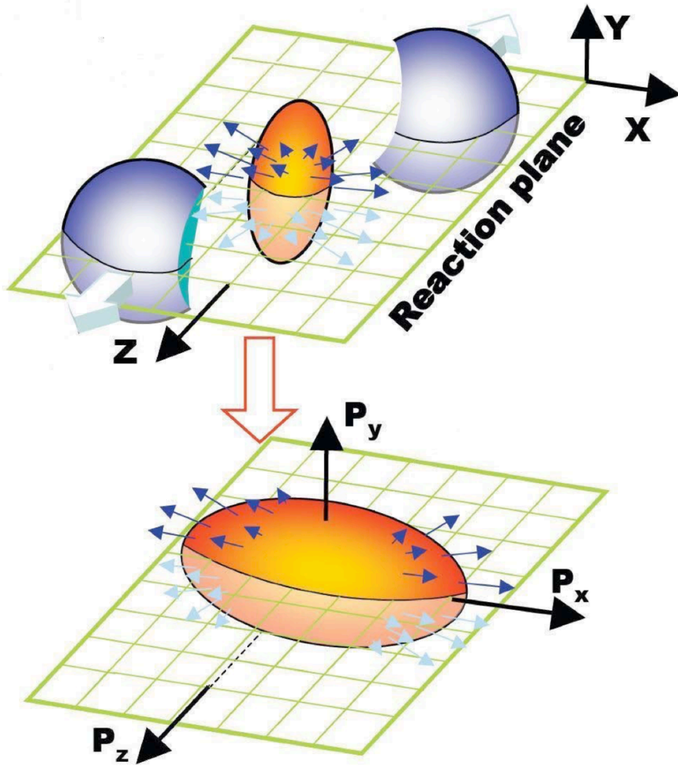

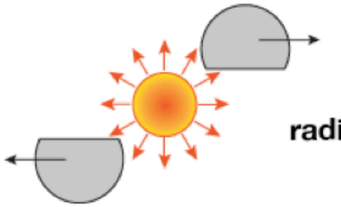

radial flow

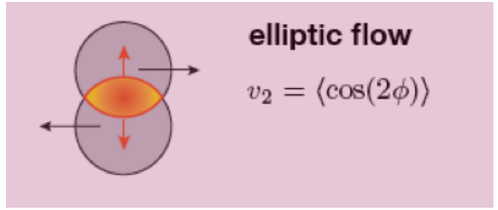

elliptic flow

$v_2 = \langle\cos(2\phi)\rangle$

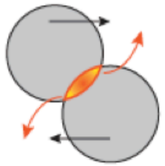

directed flow

$v_1 = \langle\cos(\phi)\rangle$

triangular flow

$v_3 = \langle\cos(3\phi)\rangle$

$\phi = (\varphi - \Psi_{RP})$

STAR: PRC 88 (2013) 14902
Phys. Rev. C 93, 014907 (2016)
Phys. Rev. Lett. 116, 062301 (2016)

$$E\frac{d^3N}{d^3\mathbf{p}} = \frac{1}{2\pi}\frac{d^2N}{p_t dp_t dy}\left(1 + 2\sum_{n=1}^{\infty} v_n \cos[n(\varphi - \Psi_{RP})]\right)$$

Elliptic flow

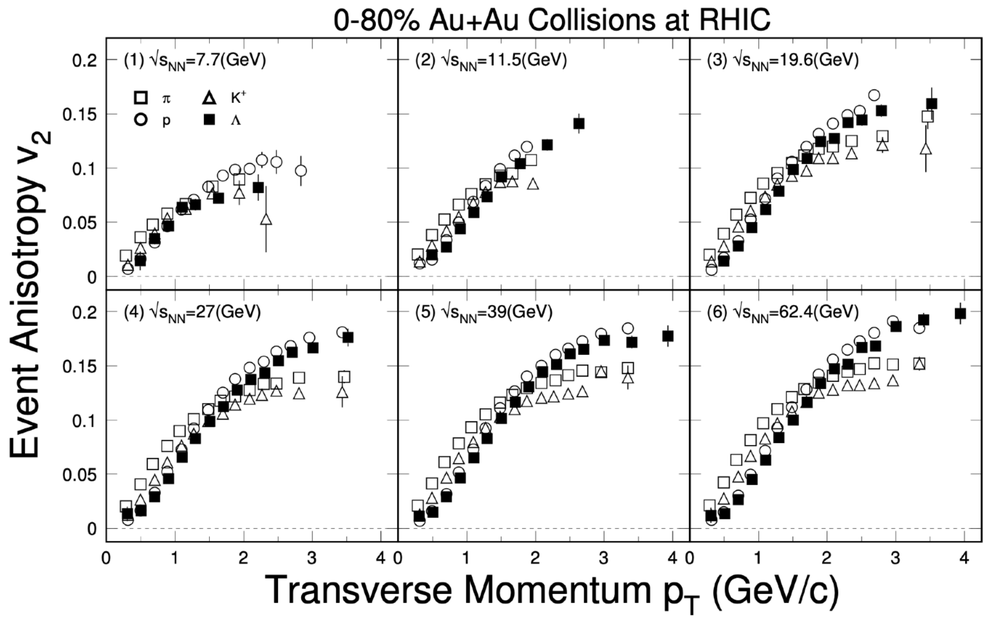

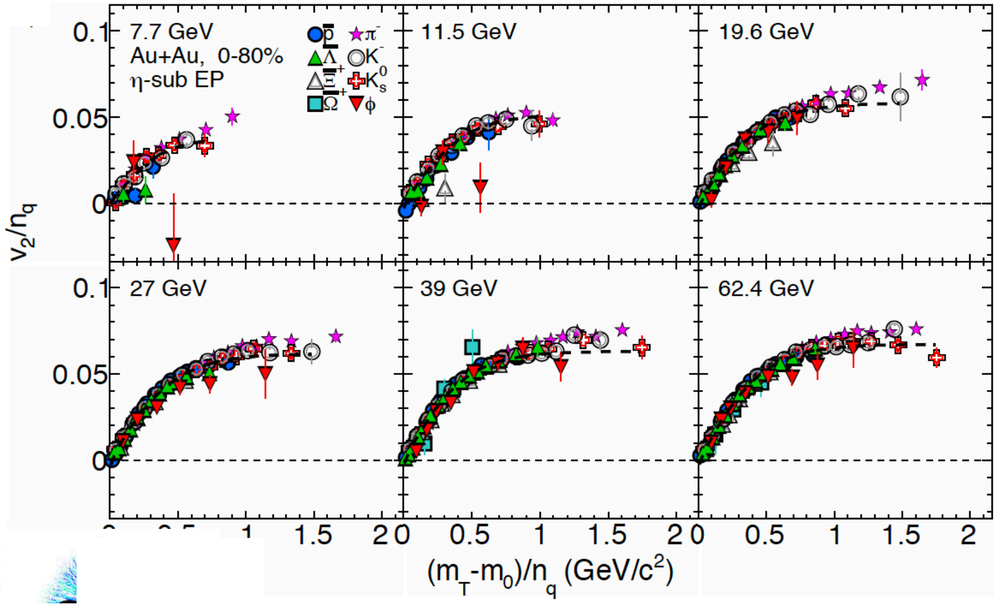

$v_2(p_T)$ are mass ordered

- ϕ meson v_2 fails the trend from other hadrons at $\sqrt{s_{NN}} = 11.5$ GeV, (low statistics)
- NCQ scaling between particles is broken ($\sqrt{s_{NN}} < 19.6$ GeV) and consistent with hadronic interactions becoming dominant

STAR: PRC 88 (2013) 14902
Phys. Rev. C 93, 014907 (2016)
Phys. Rev. Lett. 116, 062301 (2016)

Elliptic flow

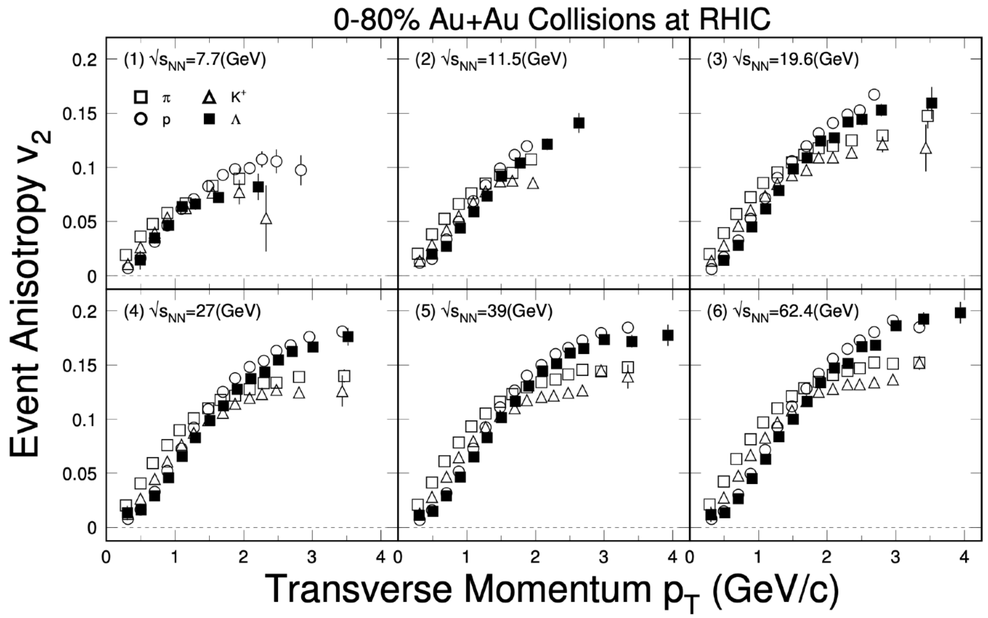

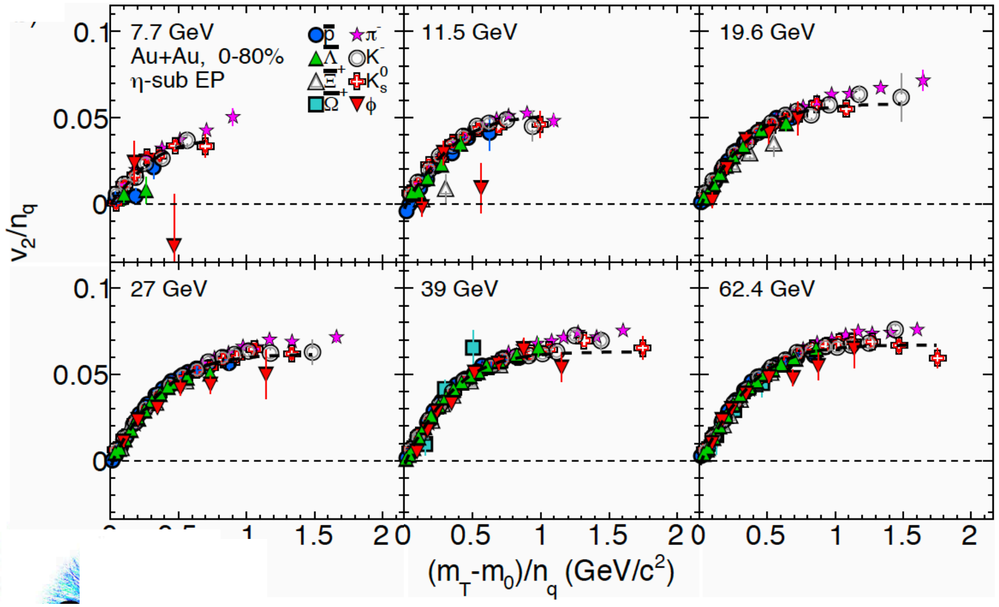

$v_2(p_T)$ are mass ordered

- ϕ meson v_2 falls the trend from other hadrons at $\sqrt{s_{NN}} = 11.5$ GeV, (low statistics)
- NCQ scaling between particles is broken ($\sqrt{s_{NN}} < 19.6$ GeV) and consistent with hadronic interactions becoming dominant

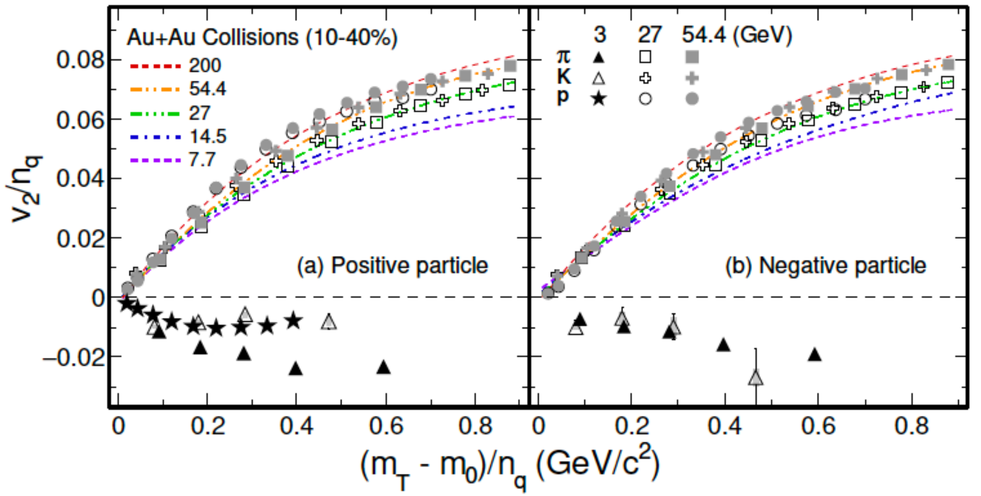

- $v_2 > 0 \rightarrow$ formation of the QGP, scaling of NCQ
- $v_2 < 0$, slope of the $v_1 < 0$ ($\sqrt{s_{NN}} = 3$ GeV) $\rightarrow$ NCQ scaling absent

STAR: PRC 88 (2013) 14902
Phys. Rev. C 93, 014907 (2016)
Phys. Rev. Lett. 116, 062301 (2016)

Elliptic flow

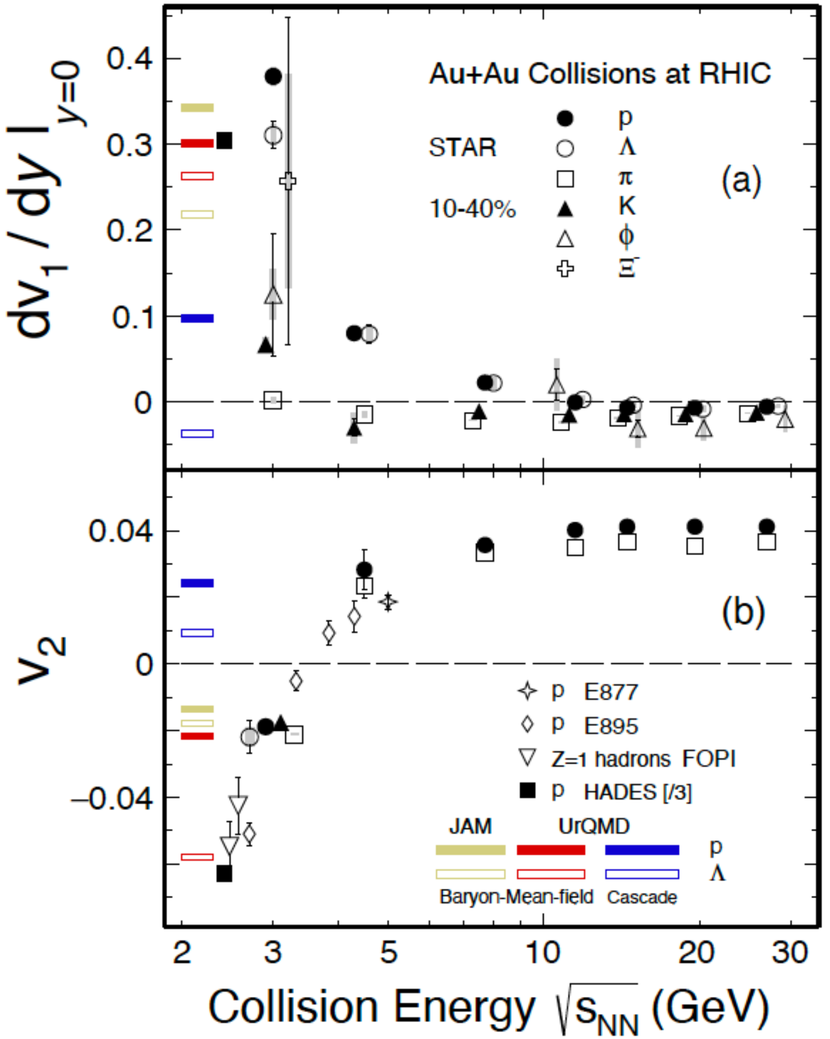

- $v_2 > 0 \rightarrow$ partonic collectivity $\rightarrow$ formation of QGP $\rightarrow$ scaling of NCQ
- $v_2 < 0$, slope of the $v_1 < 0$ ($\sqrt{s_{NN}} = 3$ GeV) $\rightarrow$ NCQ scaling absent

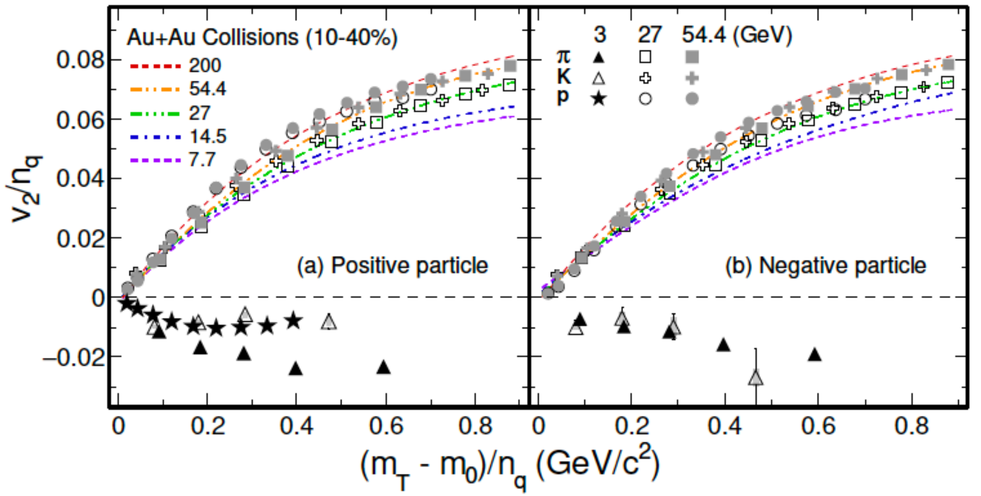

- $v_2 > 0 \rightarrow$ formation of the QGP, scaling of NCQ
- $v_2 < 0$, slope of the $v_1 < 0$ ($\sqrt{s_{NN}} = 3$ GeV) $\rightarrow$ NCQ scaling absent

- JAM, UrQMD mean field reproduced results.
- Vanishing of partonic collectivity and a new EOS, dominated by baryonic interactions in the high baryon density region.

STAR: PRC 88 (2013) 14902
Phys. Rev. C 93, 014907 (2016)
Phys. Rev. Lett. 116, 062301 (2016)

Observables

1. **Onset of QGP** (disappearance of signals of partonic degrees of freedom)
Charge separation w.r.t. EP
NCQ scaling of elliptic flow

2. Observation of **phase transition** (softening of EOS at lower collision energy)
Directed flow v_1
Femtoscopy

3. Existence of **Critical Point** (CP)
Fluctuation analyses

4. **Chiral symmetry restoration**
Low-mass vector mesons, dileptons CME

5. … and **beyond ..**
Light nuclei
Lambda's polarization
Hypernuclei production
Nuclear modification factor

Directed flow and $< m_T > - m$ dependence

- v_1 probes early stage of collision;
- v_1 sensitive to compression;
- v_1 should be sensitive to the first-order phase transition;
- change of sign in the slope of $\frac{dv_1}{dy}$ (for baryons, or net-baryons) as a probe to the softening of EOS and/or the first-order phase transition;
- If a system undergoes a first-order phase transition, due to formation of mixed phase, pressure gradient is small (minimum in the v_1 slope parameter);

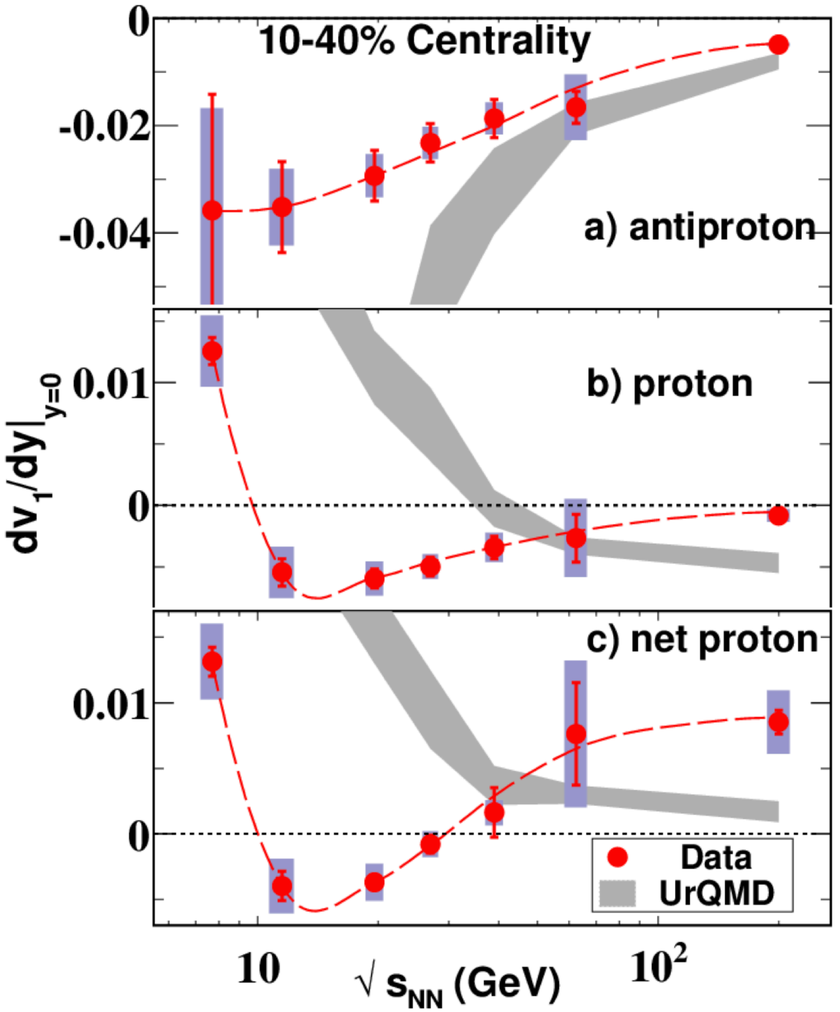

STAR, PRL 112, 162301 (2014)

Directed flow and $< m_T > - m$ dependence

- v_1 probes early stage of collision;
- v_1 sensitive to compression;
- v_1 should be sensitive to the first-order phase transition;
- change of sign in the slope of $\frac{dv_1}{dy}$ (for baryons, or net-baryons) as a probe to the softening of EOS and/or the first-order phase transition;
- If a system undergoes a first-order phase transition, due to formation of mixed phase, pressure gradient is small (minimum in the v_1 slope parameter);
- $< m_T > - m$ measures thermal excitation in the transverse direction

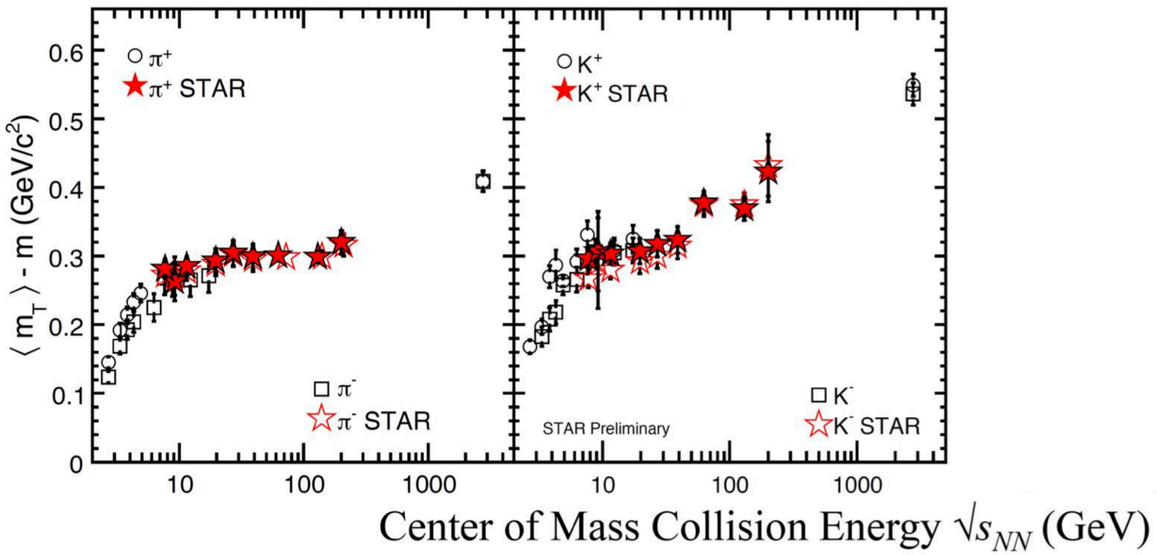

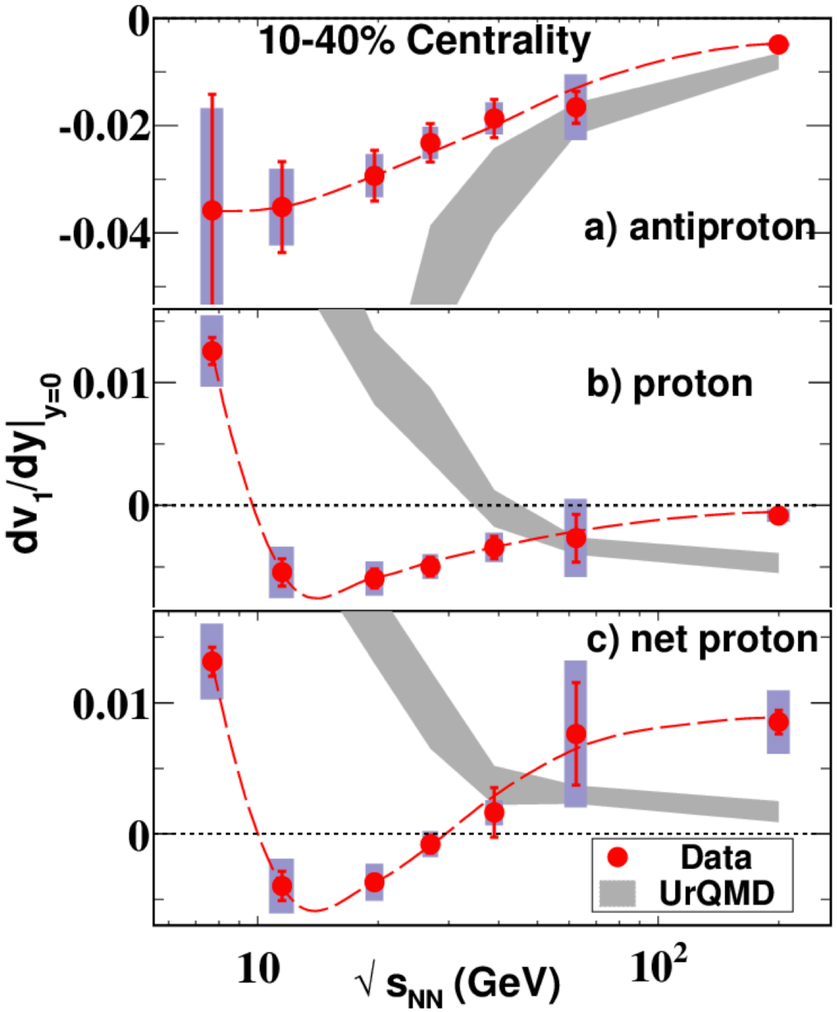

STAR, PRL 112, 162301 (2014)

Femtoscopy

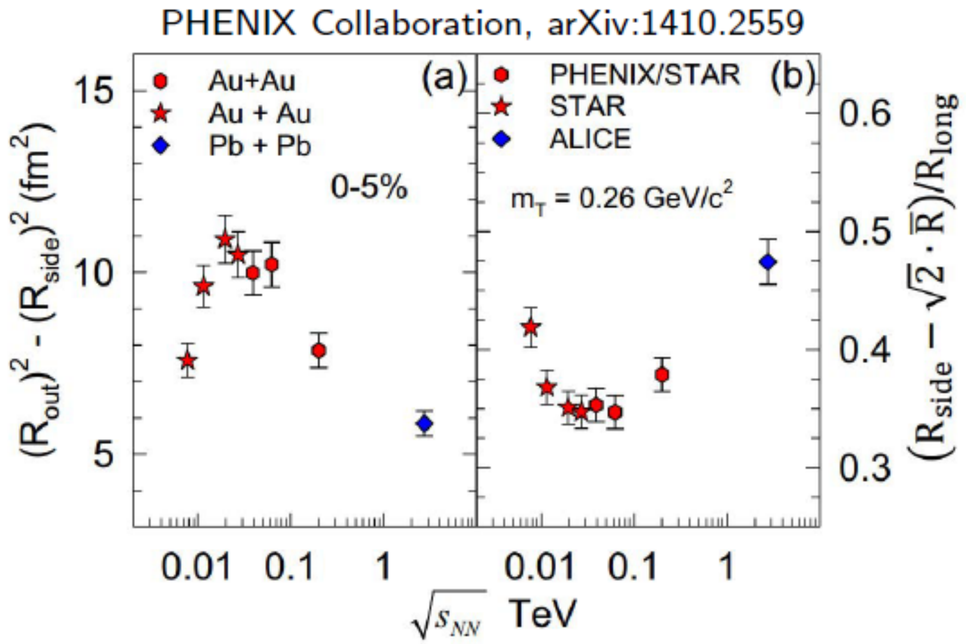

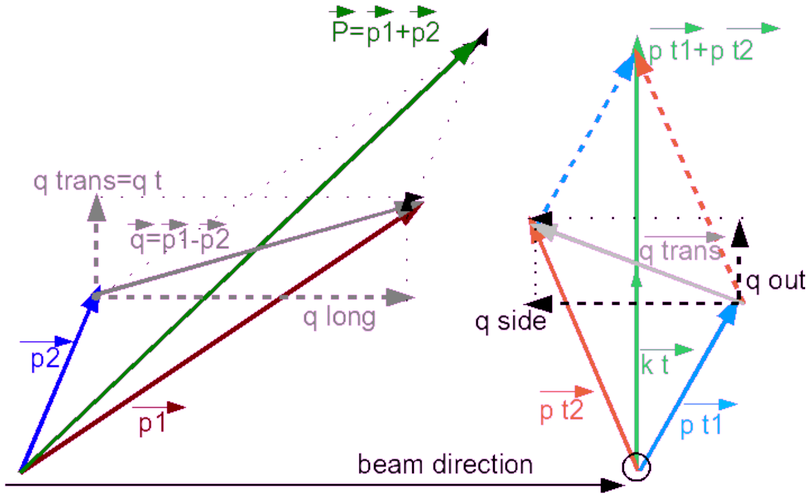

- $R_{out}^2 - R_{side}^2 = \beta_t^2 \Delta\tau^2$: related to emission duration
- $(R_{\text{side}} - \sqrt{2}\bar{R})/R_{\text{long}}$: related to expansion velocity, $\bar{R}$: initial transverse size
- Indication of the critical behavior?

Femtoscopy

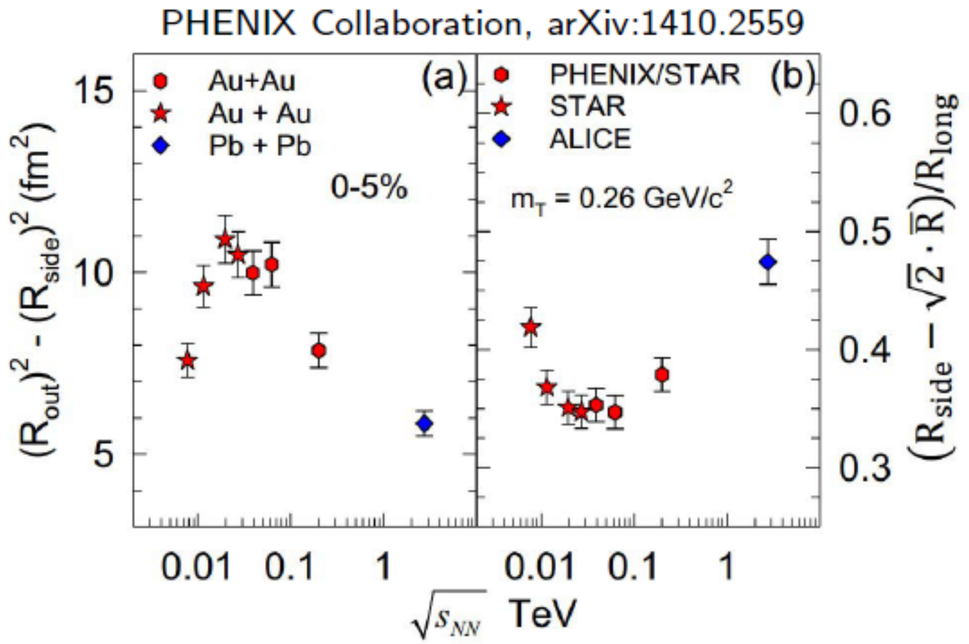

- $R_{out}^2 - R_{side}^2 = \beta_t^2 \Delta\tau^2$: related to emission duration
- $(R_{\text{side}} - \sqrt{2}\bar{R})/R_{\text{long}}$: related to expansion velocity, $\bar{R}$: initial transverse size
- Indication of the critical behavior?

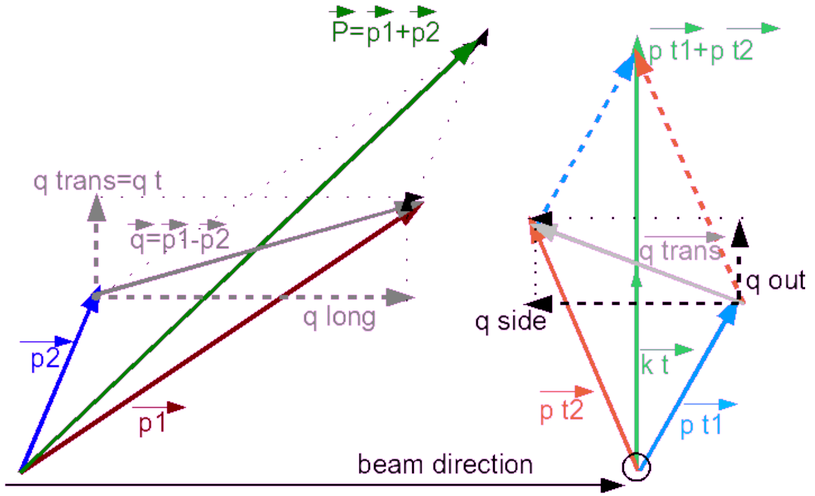

- Visible **peak** in $\frac{R_{out}}{R_{side}}(\sqrt{s_{NN}})$ near the $\sqrt{s_{NN}} \simeq$ 20 GeV
- QCD calculations predict a peak near to the QGP transition threshold - signature of first-order phase transition?
- Theoretical attention from hydro and transport models needed

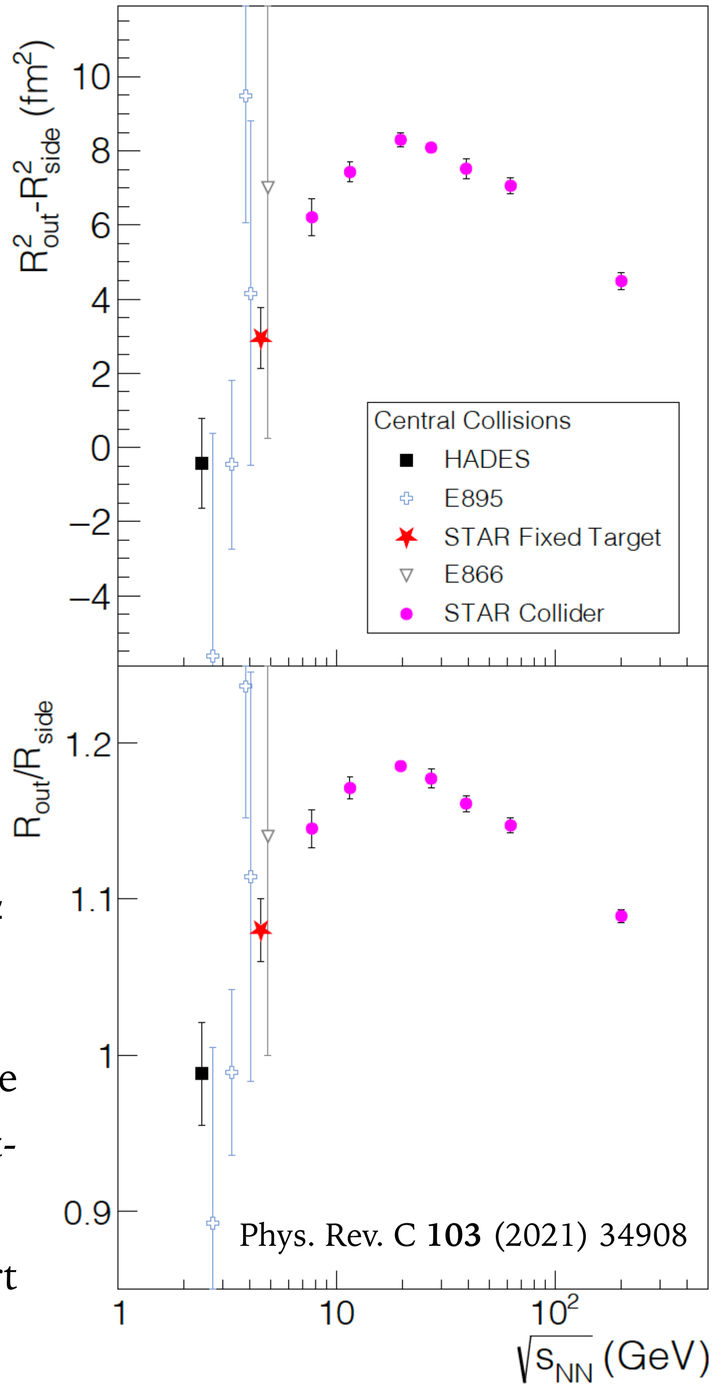

Observables

1. **Onset of QGP** (disappearance of signals of partonic degrees of freedom)
Charge separation w.r.t. EP
NCQ scaling of elliptic flow

2. Observation of **phase transition** (softening of EOS at lower collision energy)
Directed flow v_1
Femtoscopy

3. Existence of **Critical Point** (CP)
Fluctuation analyses

4. **Chiral symmetry restoration**
Low-mass vector mesons, dileptons CME

5. … and **beyond ..**
Light nuclei
Lambda's polarization
Hypernuclei production
Nuclear modification factor

Fluctuations and correlations

$$\delta N = N - \langle N \rangle$$

$$C_1 = \langle N \rangle$$

$$C_2 = \langle (\delta N)^2 \rangle = \sigma^2$$

$$C_3 = \langle (\delta N)^3 \rangle$$

$$C_4 = \langle (\delta N)^4 \rangle - 3\langle (\delta N)^2 \rangle^2$$

$$S\sigma = \frac{C_3}{C_2} \qquad \kappa\sigma^2 = \frac{C_4}{C_2}$$

$$C_2 \sim \xi^2 \quad C_3 \sim \xi^{4.5} \quad C_4 \sim \xi^7$$

The higher cumulant order, the more sensitive to the correlation length

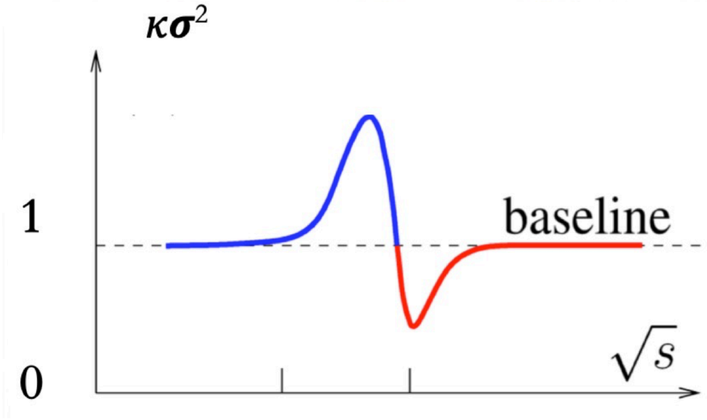

4th order: predicts a non-monotonic energy dependence due to contribution from QCD critical point

- Near the QCD CP the divergence of the correlation length expected
- Non-monotonic correlations and fluctuations related to conserved quantities (B, Q, S) could indicate CP

- Higher moments of conserved quantities measure non-Gaussian nature of fluctuations, and are more sensitive (than e.g. variance) to CP fluctuations (leads to correlation length)

Fluctuations and correlations

$$\delta N = N - \langle N \rangle$$

$$C_1 = \langle N \rangle$$

$$C_2 = \langle (\delta N)^2 \rangle = \sigma^2$$

$$C_3 = \langle (\delta N)^3 \rangle$$

$$C_4 = \langle (\delta N)^4 \rangle - 3\langle (\delta N)^2 \rangle^2$$

$$S\sigma = \frac{C_3}{C_2} \qquad \kappa\sigma^2 = \frac{C_4}{C_2}$$

$$C_2 \sim \xi^2 \quad C_3 \sim \xi^{4.5} \quad C_4 \sim \xi^7$$

The higher cumulant order, the more sensitive to the correlation length

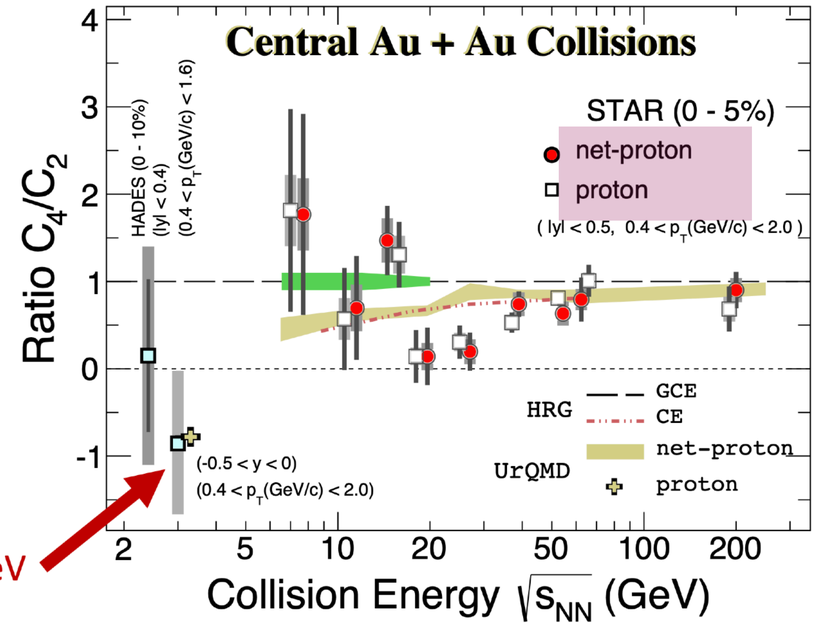

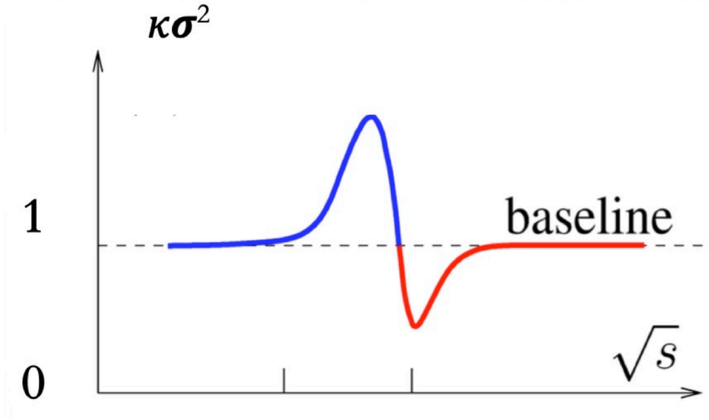

4th order: predicts a non-monotonic energy dependence due to contribution from QCD critical point

- Near the QCD CP the divergence of the correlation length expected
- Non-monotonic correlations and fluctuations related to conserved quantities (B, Q, S) could indicate CP

- Higher moments of conserved quantities measure non-Gaussian nature of fluctuations, and are more sensitive (than e.g. variance) to CP fluctuations (leads to correlation length)

- Non-monotonic energy dependence of net- proton consistent with theoretical expectation with a CP.
- The suppression of C4/C2 consistent with fluctuations driven by baryon number conservation indicating a hadronic interaction dominated region at $\sqrt{s_{NN}} = 3$ GeV
- The QCD critical point, (if exists in heavy ion collisions), could be located at $\sqrt{s_{NN}} > 3$ GeV; STAR, PRL 126, 092301 (2021), PRC 104.024902 (2021), PRL 128.202303 (2022)

Observables

1. **Onset of QGP** (disappearance of signals of partonic degrees of freedom)
Charge separation w.r.t. EP
NCQ scaling of elliptic flow

2. Observation of **phase transition** (softening of EOS at lower collision energy)
Directed flow v_1
Femtoscopy

3. Existence of **Critical Point** (CP)
Fluctuations analyses

4. **Chiral symmetry restoration**
Low-mass vector mesons, dileptons CME

5. … and **beyond ..**
Light nuclei
Lambda's polarization
Hypernuclei production
Nuclear modification factor

Thermal dileptons at BES

Hadrons (yields, p_T) -> Statistical thermal models -> T_{ch}

-> Hydro-inspired models -> T_k

- EM probes (photons, leptons): emitted from early to final stages of HIC, carry original information of emission source, probe earlier and hotter phases of medium

- Why dileptons?
  Mass spectral of thermal dileptons could reveal temperature of the hot medium at both QGP phase and hadronic phase

- How to measure thermal dileptons?
  Interested signal (in medium ρ decays, QGP radiation) + **Physics background** (cocktails) = **Inclusive signal** (space-time integral)

Thermal dileptons at BES

Hadrons (yields, p_T) -> Statistical thermal models -> T_{ch}

-> Hydro-inspired models -> T_k

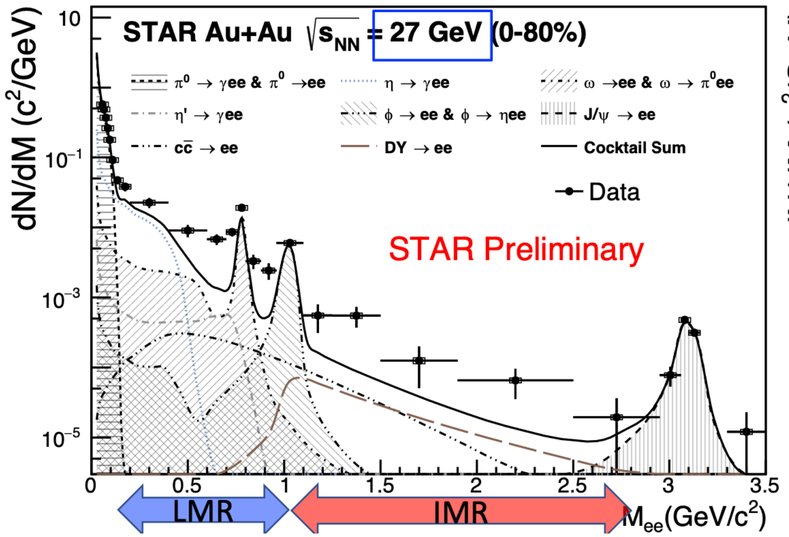

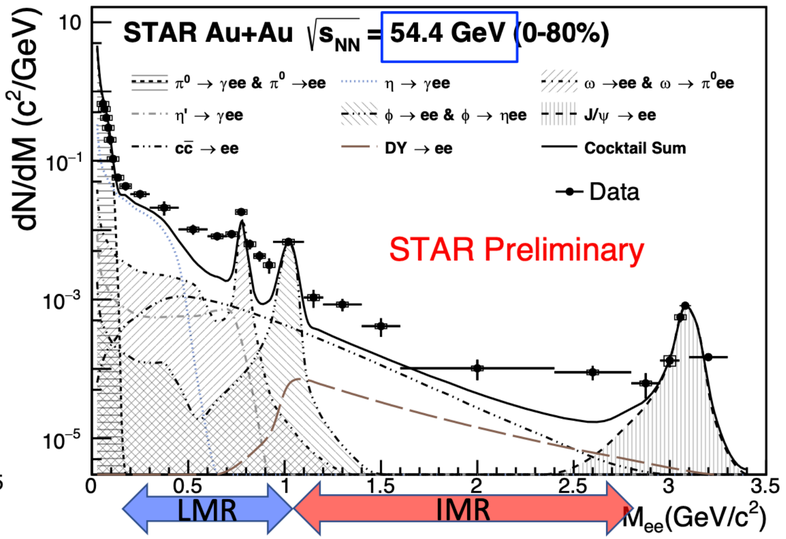

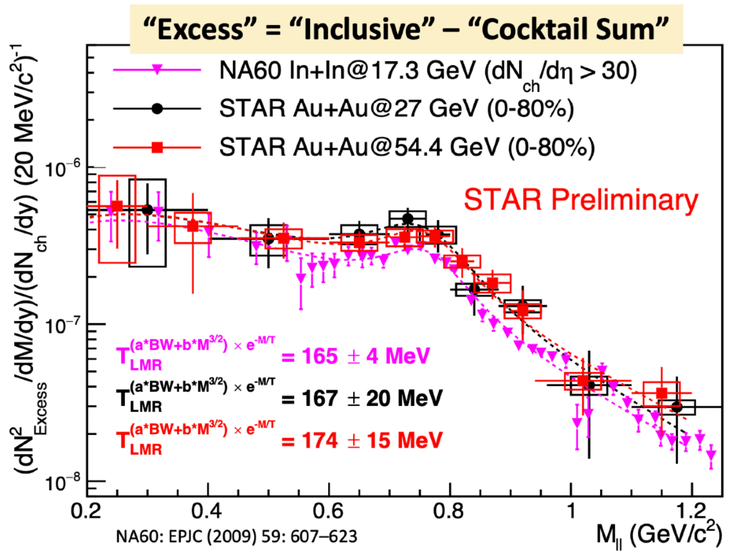

T are similar, despite significant difference in collision species and energies, indicate that ρ **is dominantly emitted around phase transition**

- EM probes (photons, leptons): emitted from early to final stages of HIC, carry original information of emission source, probe earlier and hotter phases of medium

- Why dileptons?
  Mass spectral of thermal dileptons could reveal temperature of the hot medium at both QGP phase and hadronic phase

- How to measure thermal dileptons?
  Interested signal (in medium ρ decays, QGP radiation) + **Physics background** (cocktails) = **Inclusive signal** (space-time integral)

Thermal dileptons at BES

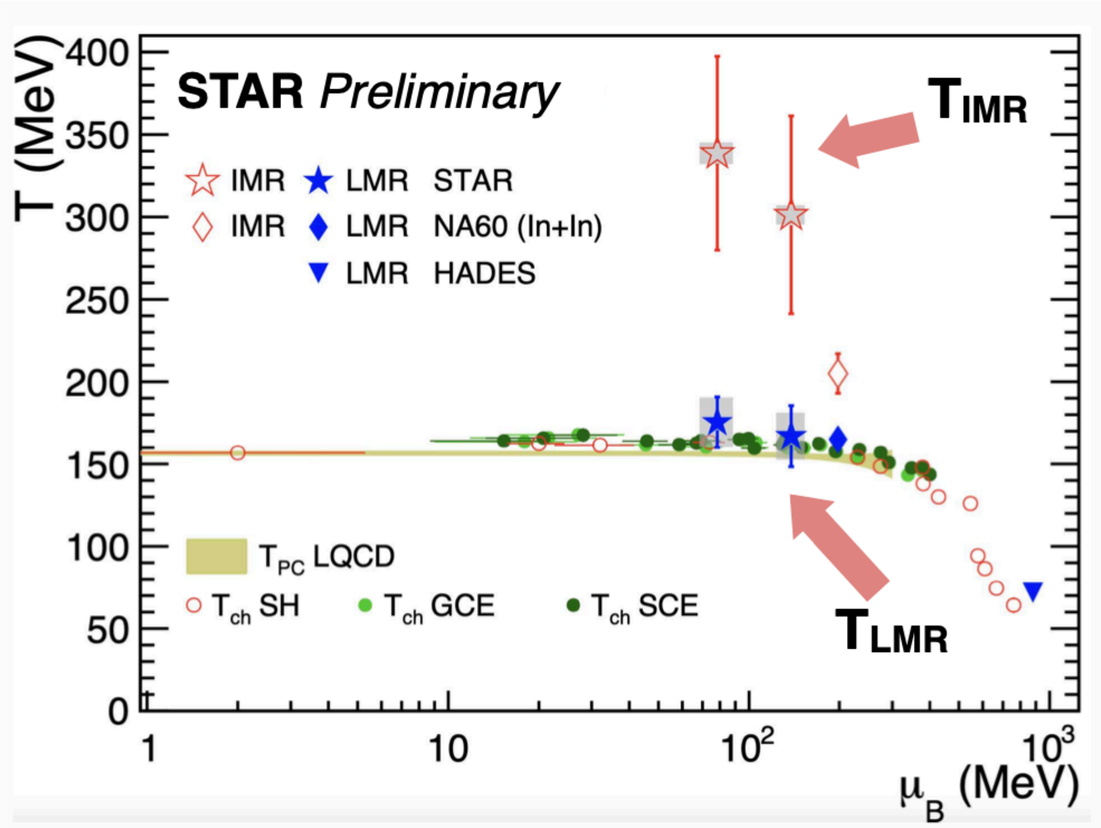

Thermal dileptons in IMR

- T always higher than phase transition T at RHIC and SPS
- Emitted from QGP phase

Thermal dileptons in LMR

- T consistent with T_{ch} from statistical models
- Emitted from hadronic phase, dominantly around phase transition region at RHIC and SPS

Thermal dileptons at BES

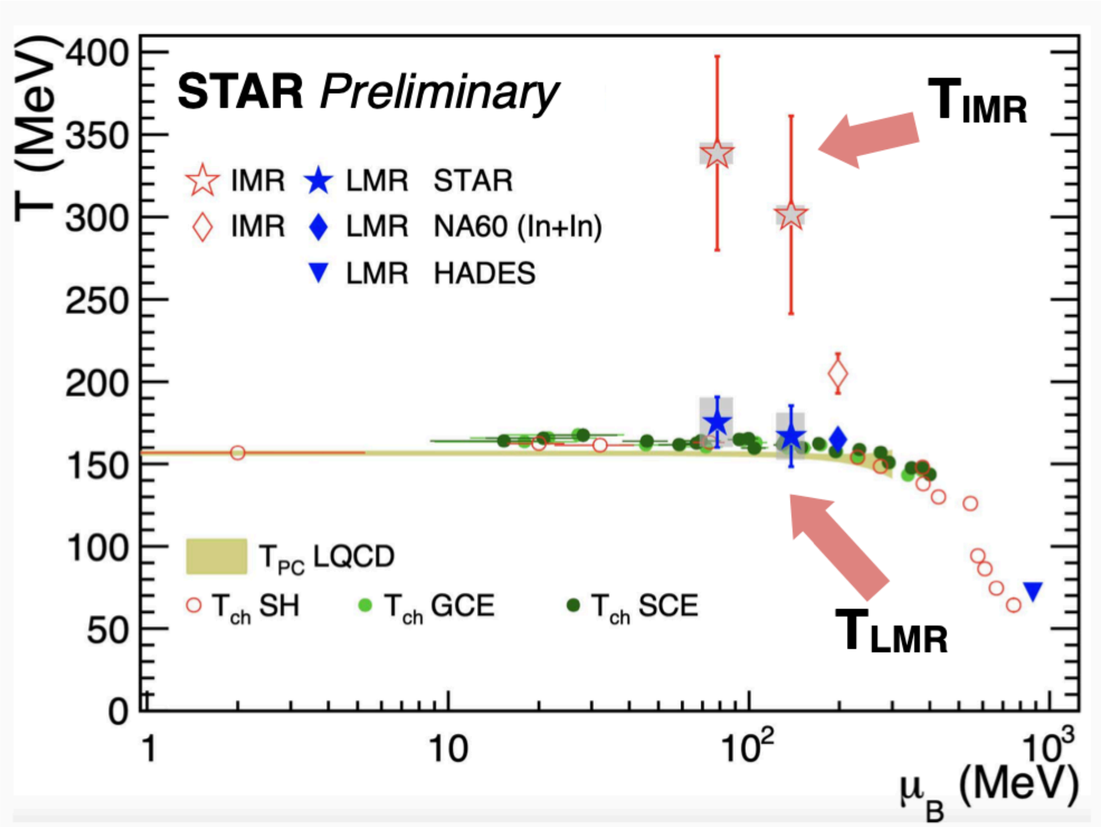

T_{IMR} ~ **300 MeV**: First **QGP** temperature measurement at RHIC

QGP produced at RHIC is hotter than that at SPS

Thermal dileptons in IMR

- T always higher than phase transition T at RHIC and SPS
- Emitted from QGP phase

Thermal dileptons in LMR

- T consistent with T_{ch} from statistical models
- Emitted from hadronic phase, dominantly around phase transition region at RHIC and SPS

- T_{LMR} ~ **170 MeV**: First experimental evidence that in-medium ρ (hadronic matter) is dominantly produced around temperature higher than T at the phase transition
- Normalized dilepton yield is higher in RHIC Au+Au than that in SPS In+In: indicate a longer medium lifetime for larger collision systems

Summary from BES

Continue to look for the **Critical Point** and
the **first-order phase transition**.

Data exists over wide range of the collision energy for heavy and light ions, p(d), and pp

High statistics exploration of QCD phase diagram and its key features has already begun

More coming soon (BES-II, SPS, FAIR)

Turn trends and features into definite conclusions

More interesting questions appeared..

Summary from BES

Continue to look for the **Critical Point** and
the **first-order phase transition**.

Data exists over wide range of the collision energy for heavy and light ions, p(d), and pp

High statistics exploration of QCD phase diagram and its key features has already begun

More coming soon (BES-II, SPS, FAIR)

Turn trends and features into definite conclusions

More interesting questions appeared..

Thank You for your attention!

- 3.83 km circumference
- Two independent rings
- Collides so far:
  - Au+Au, p+p, d+Au, Cu+Cu, U+U, Cu+Au, ^{3}He+Au, p+Au
- Top Center-of-Mass Energy
  - 510 GeV for p-p
  - 200 GeV/nucl. for Au-Au

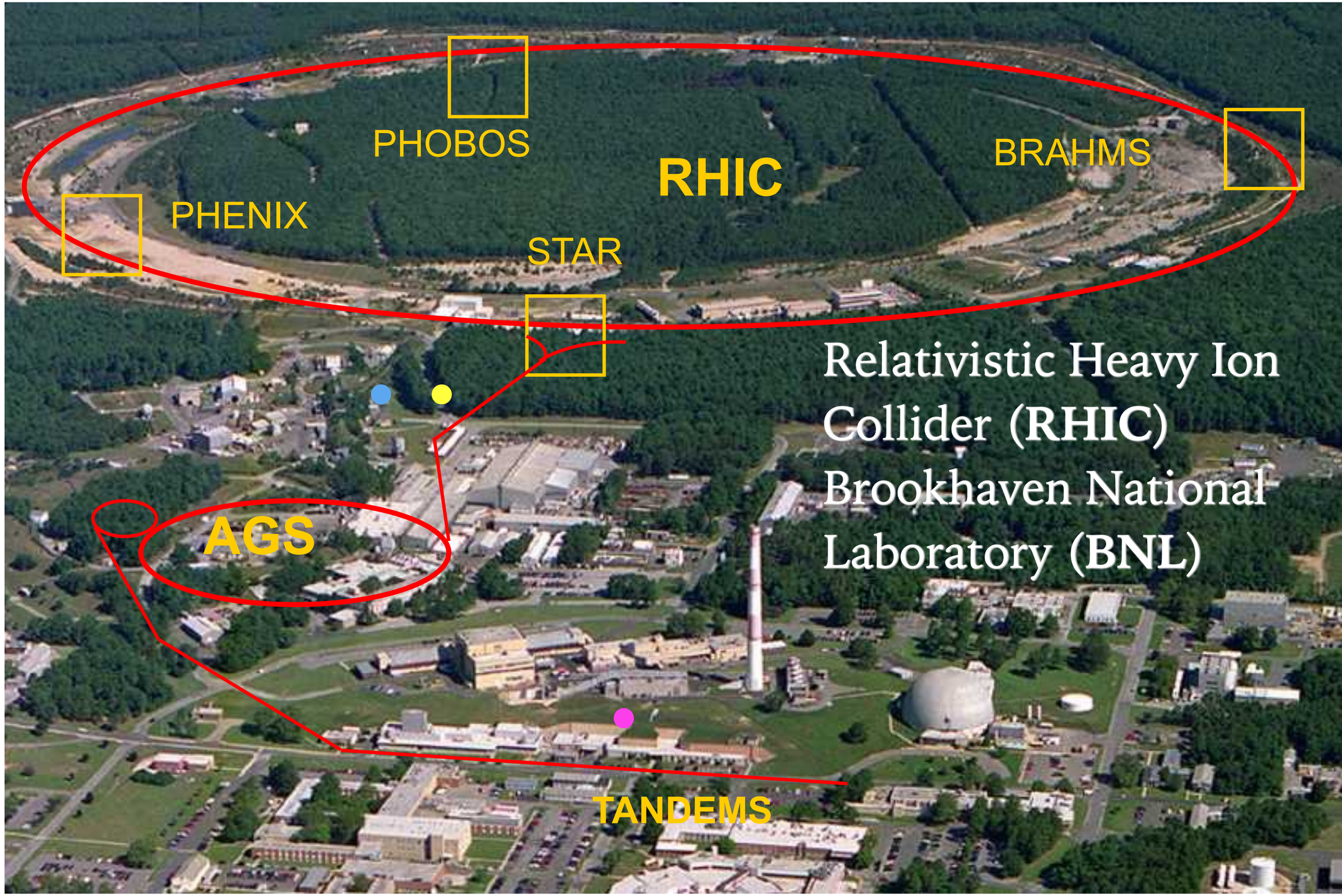

Particle identification

arXiv:2007.14005 (STAR)

$\sqrt{s_{NN}}$=4.5GeV Fixed Target

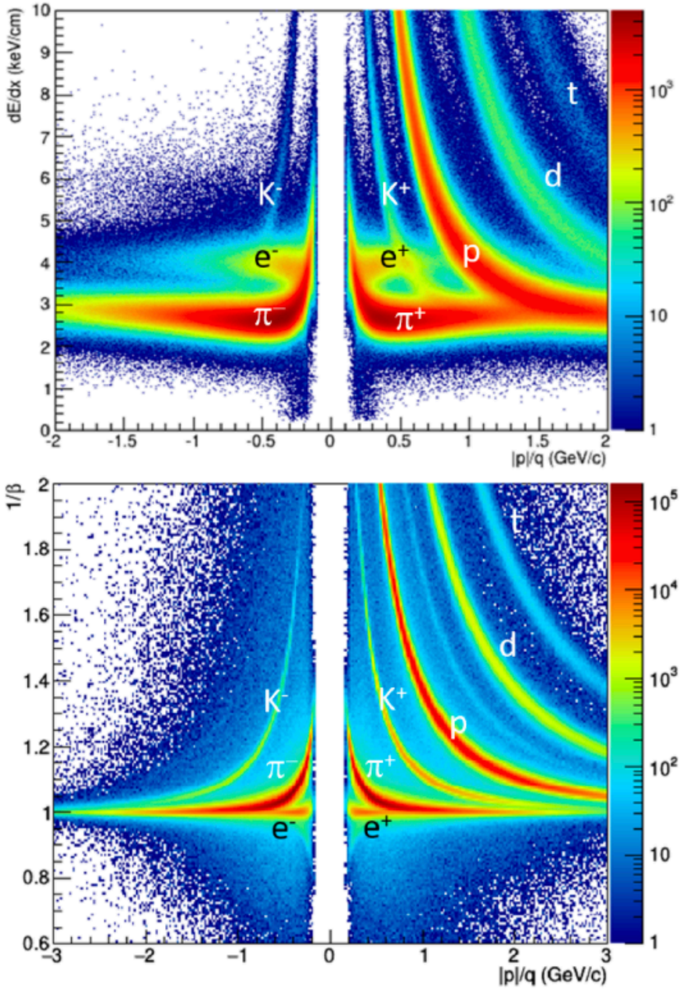

PRC 101 (2020) 24905 (STAR)

$\sqrt{s_{NN}}$=14.5GeV Collider

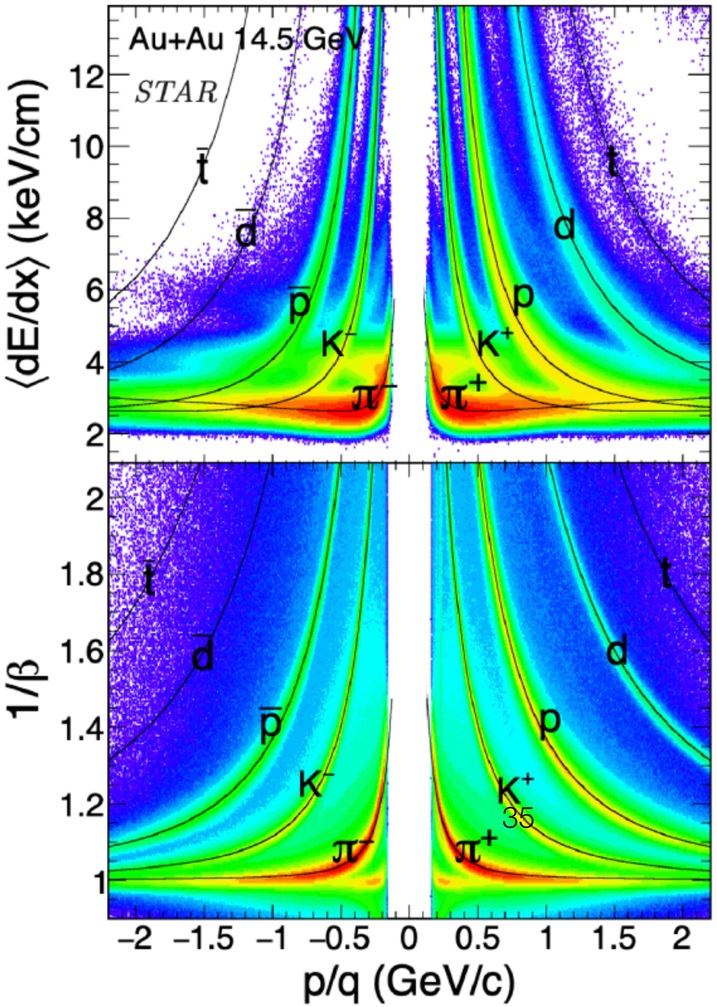

PRC 102 (2020) 34909 (STAR)

$\sqrt{s_{NN}}$=7.7GeV Collider

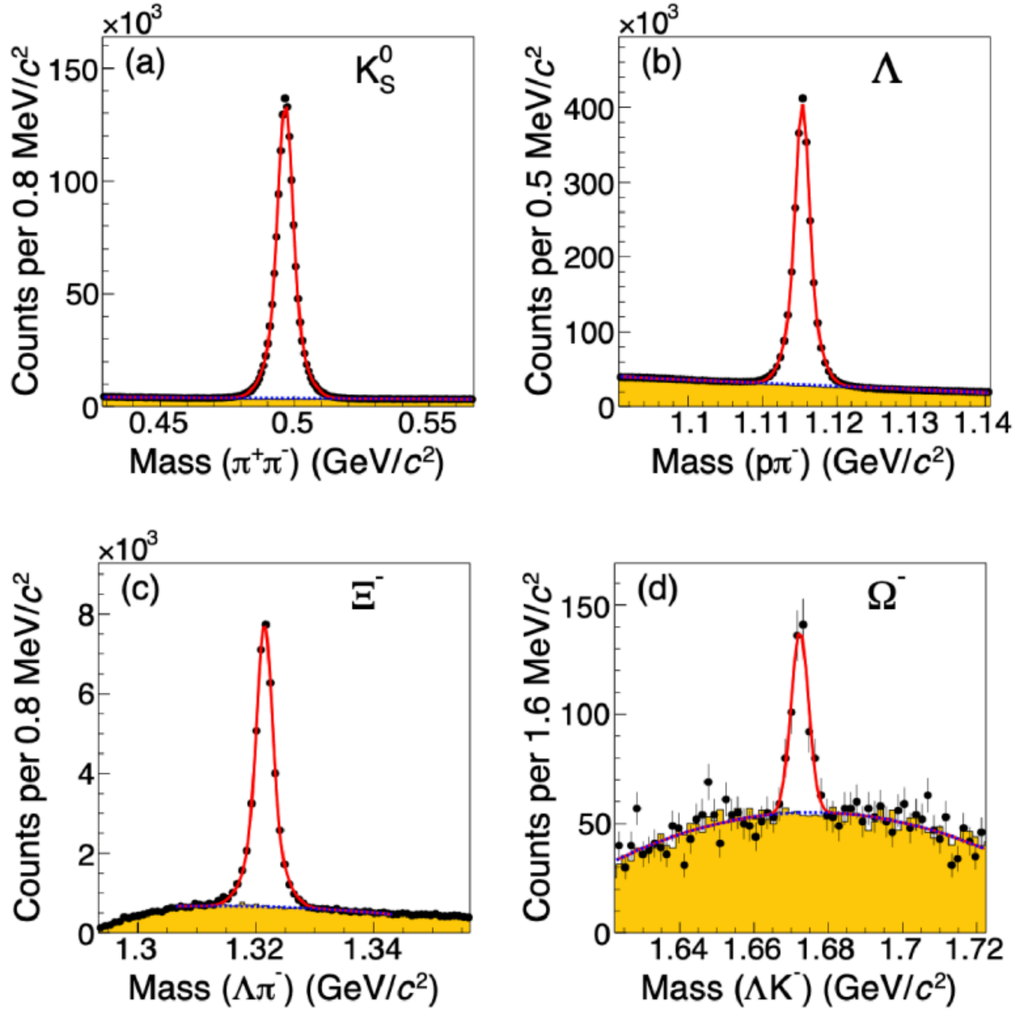

Collider and fixed-target acceptance

Au+Au at 7.7 GeV

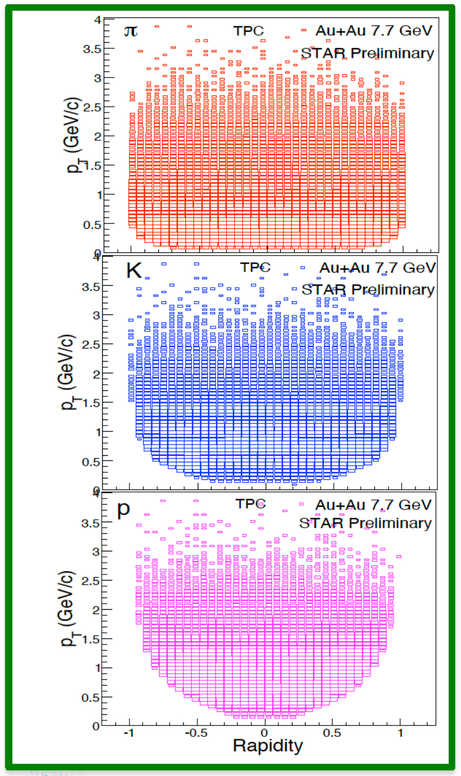

Au+Au at *39* GeV

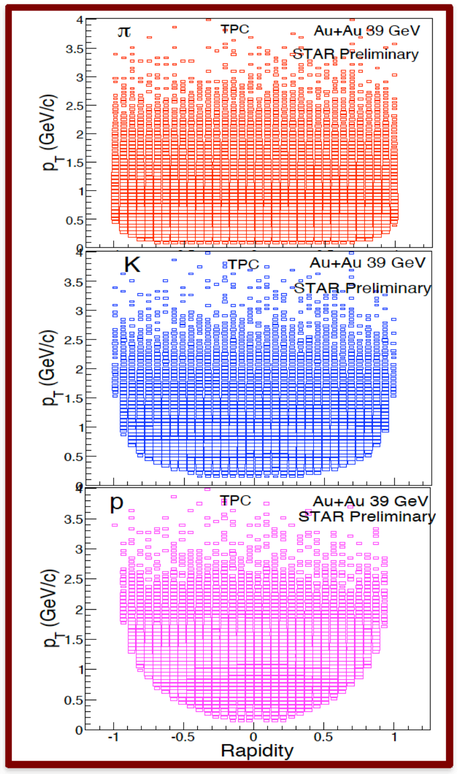

Au+Au at *200* GeV

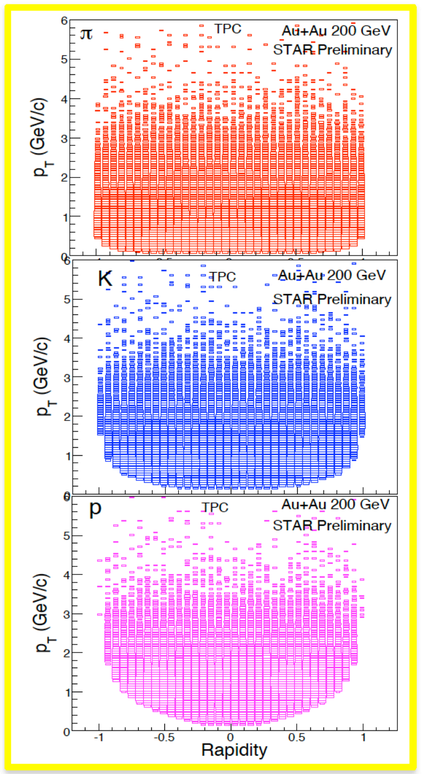

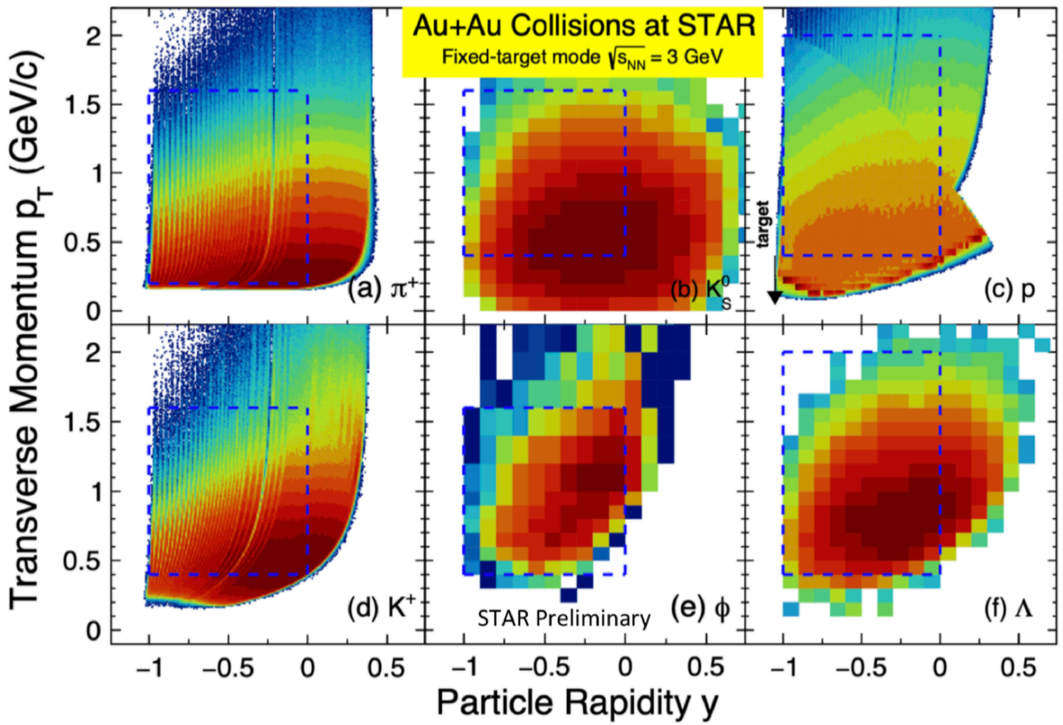

Similar acceptance for all particles and energies

R_{CP} for charged particles

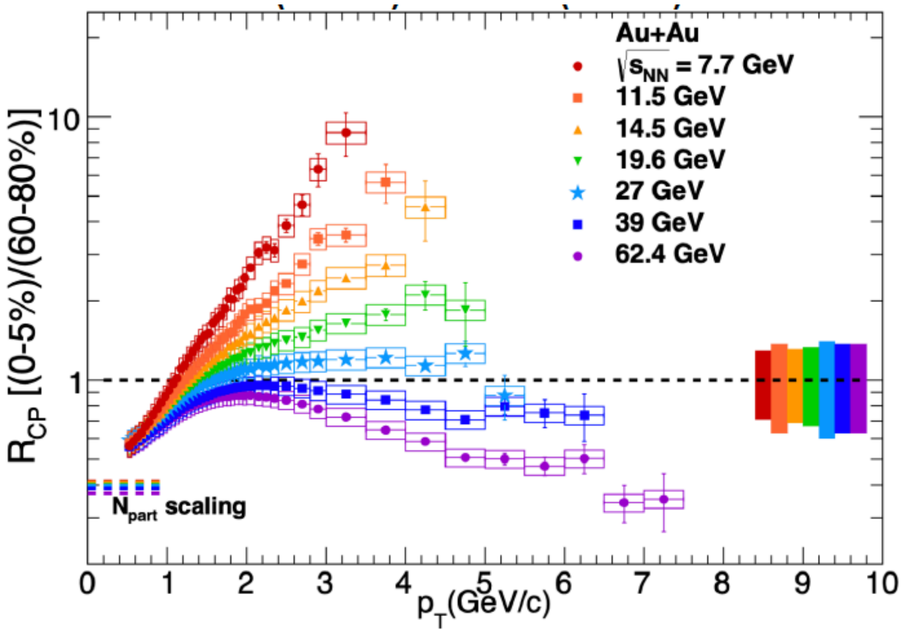

PRL 121 (2018) 32301 (STAR)

$$R_{CP} = \frac{< N_{bin}^{per} > d^3N_{AA}^{cen}/d\eta d^2p_T}{< N_{bin}^{cen} > d^3N_{AA}^{per}/d\eta d^2p_T}$$

increases from suppression at $\sqrt{s_{NN}}$ = 62.4 GeV to enhancement at $\sqrt{s_{NN}}$ = 7.7 GeV.

Suppression $R_{CP} < 1$: opacity of deconfinement medium of quarks and gluons.

Enhancement $R_{CP} > 1$: dominance of hadronic interactions: Cronin effect, cold matter effect, radial flow, …

$R_{CP} > 1$ does not mean that QGP is not formed.

Lack of baseline $p + p$ **and** $p + A$ **measurements**

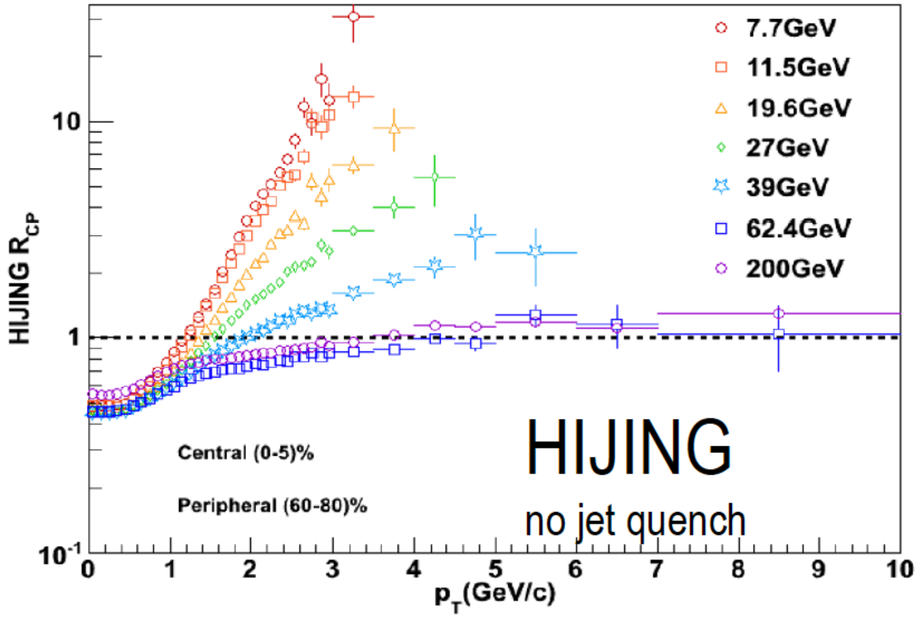

HIJING (including Cronin effect) similar to $\sqrt{s_{NN}}$ dependence at low energies

Higher order cumulants

$$\delta N = N - < N >$$
$$C_1 = < N >$$
$$C_2 = < (\delta N)^2 > = \sigma^2$$
$$C_3 = < (\delta N)^3 >$$
$$C_4 = < (\delta N)^4 > - 3 < (\delta N)^2 >^2$$
$$S\sigma = \frac{C_3}{C_2} \qquad \kappa\sigma^2 = \frac{C_4}{C_2}$$

Factorial cumulants:

$$\kappa_1 = C_1$$
$$\kappa_2 = -C_1 + C_2$$
$$\kappa_3 = 2C_1 - 3C_2 + C_3$$
$$\kappa_4 = -6C_1 + 11C_2 - 6C_3 + C_4$$
$$\kappa_5 = 24C_1 - 50C_2 + 35C_3 - 10C_4 + C_5$$
$$\kappa_6 = -120C_1 + 27C_2 - 225C_3 + 85C_4 - 15C_5 + C_6$$

Cross-over: $C_5, C_6 < 0$ - LQCD, FRG

No transition: $C_5, C_6 > 0$ - HRG, UrQMD

First order phase transition:

- multiplicity distribution bi-modal (contribution from two phases)
- $\kappa_{n+1}/\kappa_n < 0$ for higher orders

$$C_5 = < (\delta N)^5 > - 5 < (\delta N)^3 > < (\delta N)^2 >$$
$$C_6 = < (\delta N)^6 > - 15 < (\delta N)^4 > < (\delta N)^2 > - 10 < (\delta N)^3 >^2 + 30 < (\delta N)^2 >^3$$

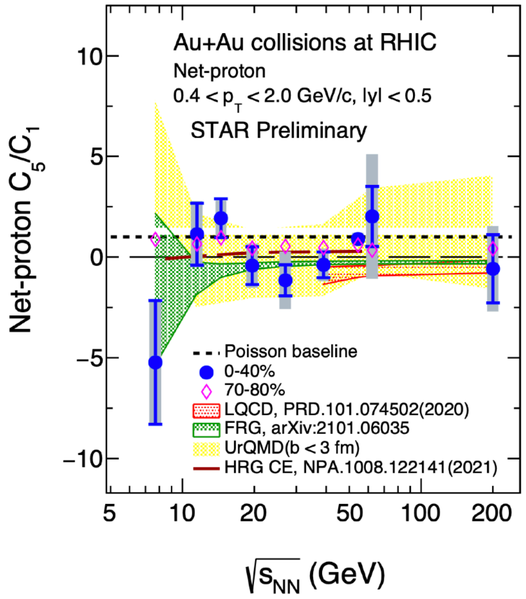

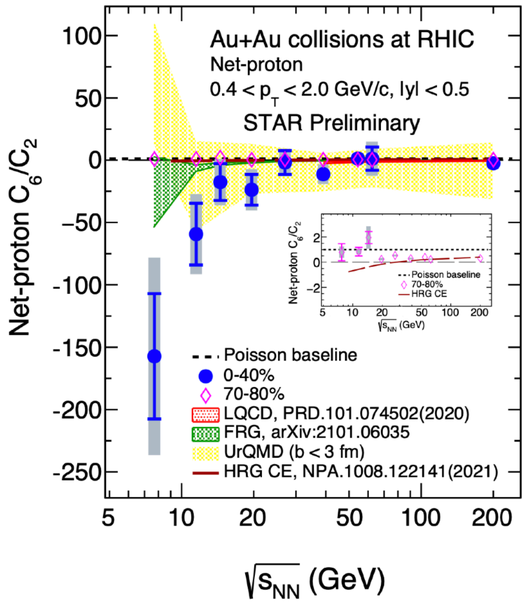

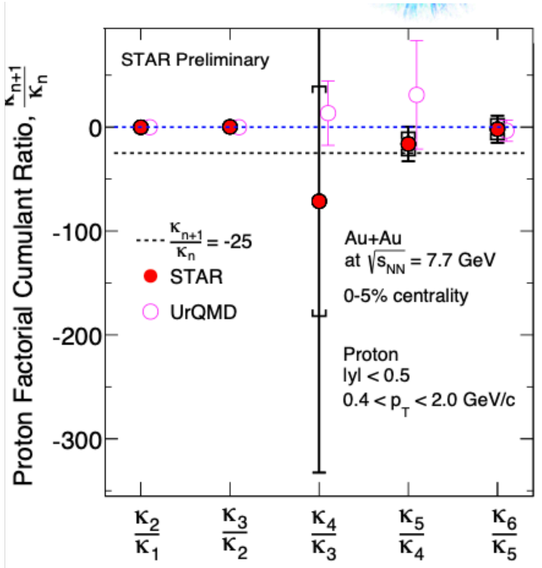

κ_5/κ_4 and κ_6/κ_5 consistent with zero.

High order fluctuations are crucial for determining the QCD phase structure. Precision measurements are necessary in order to confirm the observed trend in the fifth and sixth order cumulants.

Light nuclei

1. Light nuclei carry information about local baryon density fluctuations

2. It provides a probe to study first-order phase phase transition and the QCD Critical Point

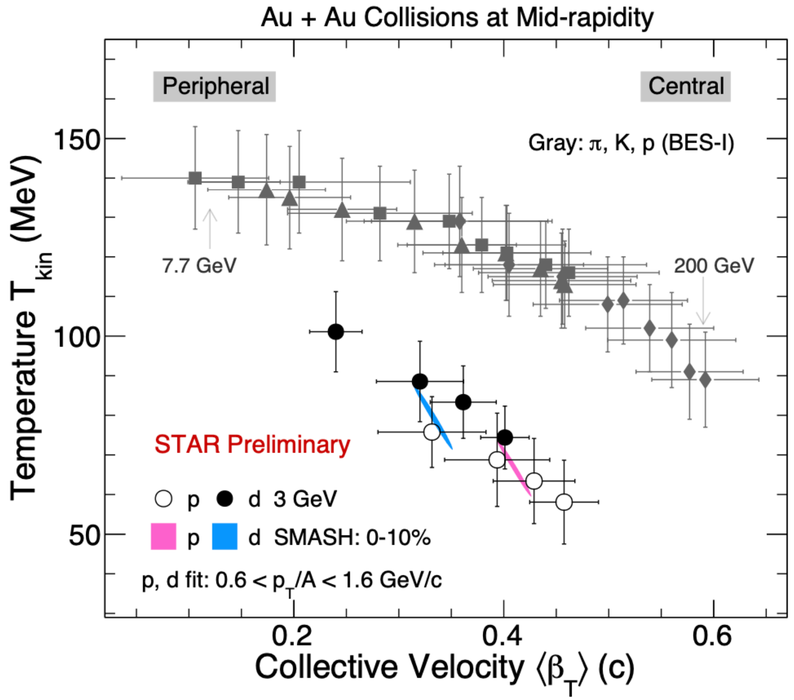

$\sqrt{s_{NN}}$ = 3 GeV collisions: First measurements of yields of p and light nuclei (d, t, ^{3}He, ^{4}He)

The freeze-out parameters show different trend compared to that of higher energy collisions: $T_{kin}(d) > T_{kin}(p)$,

Hot and dense medium created at $\sqrt{s_{NN}}$ = 3 GeV collisions seem different from that of high energy collisions

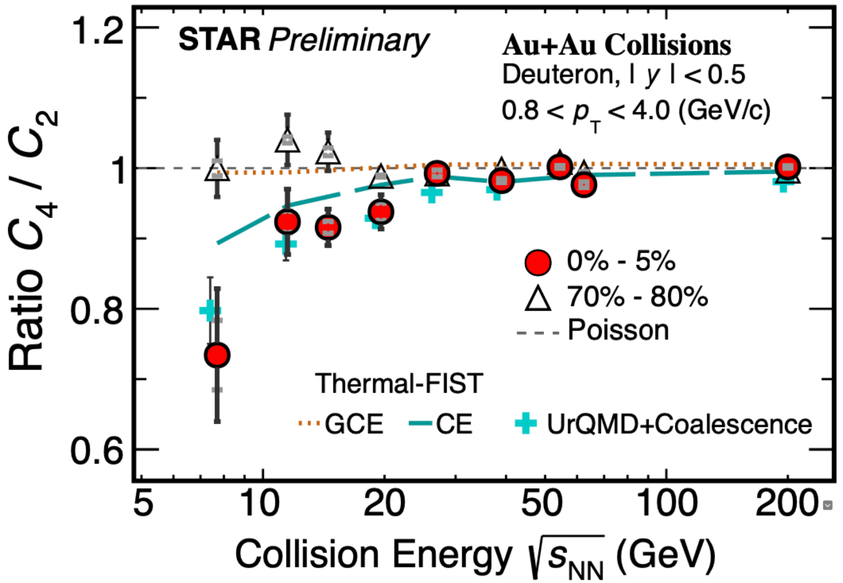

- Difference with net-proton: role of different freeze-out and smaller yield of deuterons should be investigated,
- With lowering the collision energy, C_4/C_2 is decreasing,
- **UrQMD+Coalescence model reproduces collision energy dependence.**

Hyperon polarization at BES

In non-central heavy-ion collisions large orbital momentum: $\vec{L} = \vec{r} \times \vec{p} \sim bA\sqrt{s_{NN}}$ can polarize quarks due to „spin-orbit" interaction leading to non-zero polarization of produced particles along with $\vec{L}$

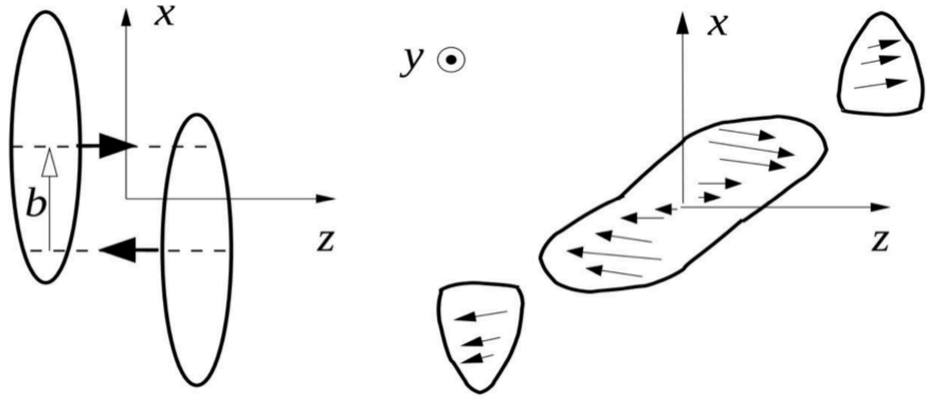

Z.-T. Liang and X.-N. Wang, Phys. Rev. Lett. 94, 102301 (2005), Erratum:ibid. 96, 039901 (2006).

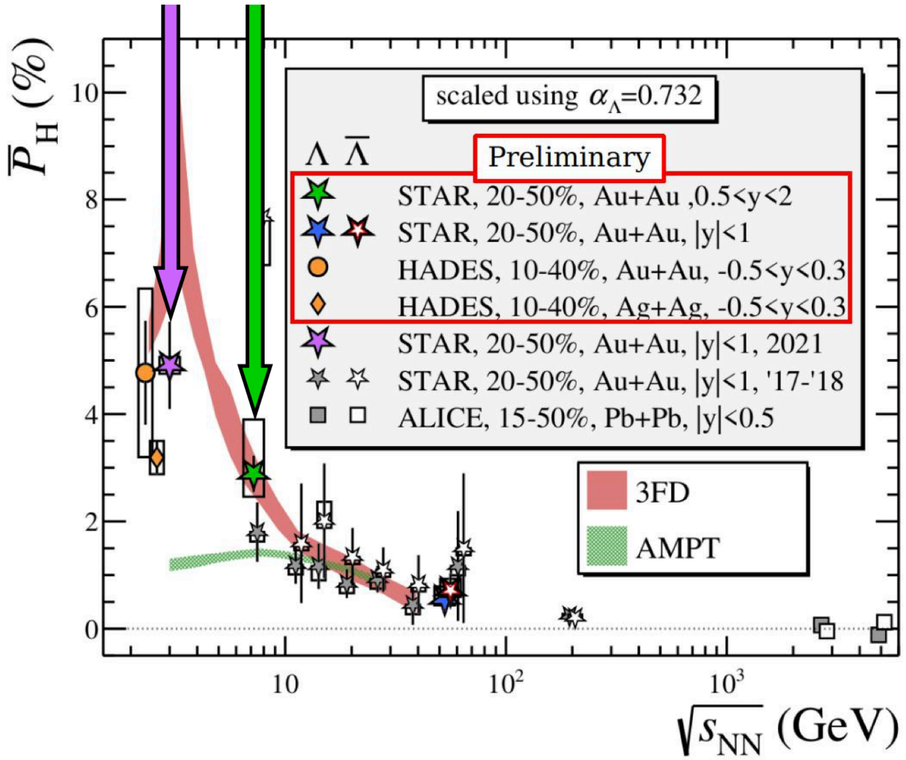

$\sqrt{s_{NN}} = 7.7$ GeV: polarization consistent with 3FD

$\sqrt{s_{NN}} = 3.0$ GeV: trend of increasing polarization persist

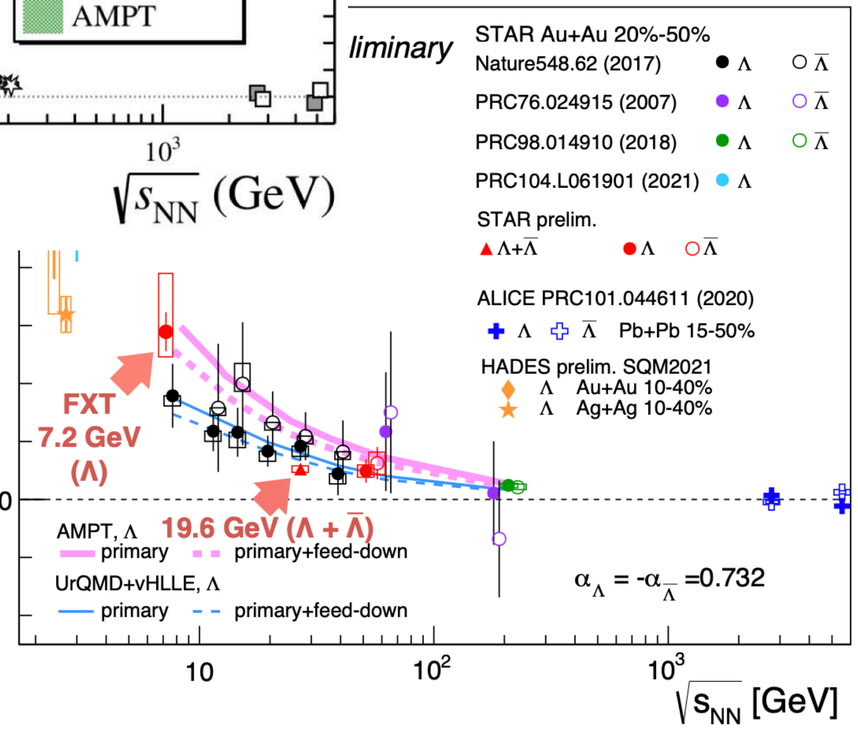

Hypernuclei production

- Provides access to the hyperon–nucleon (Y-N) interaction, strangeness in high density nuclear matter: EOS of neutron star, hadronic phase of a heavy ion collision.

- Understanding hypernuclear structure may give more constraints on the Y-N interaction. The formation of loosely bound states in heavy-ion collisions are not well understood

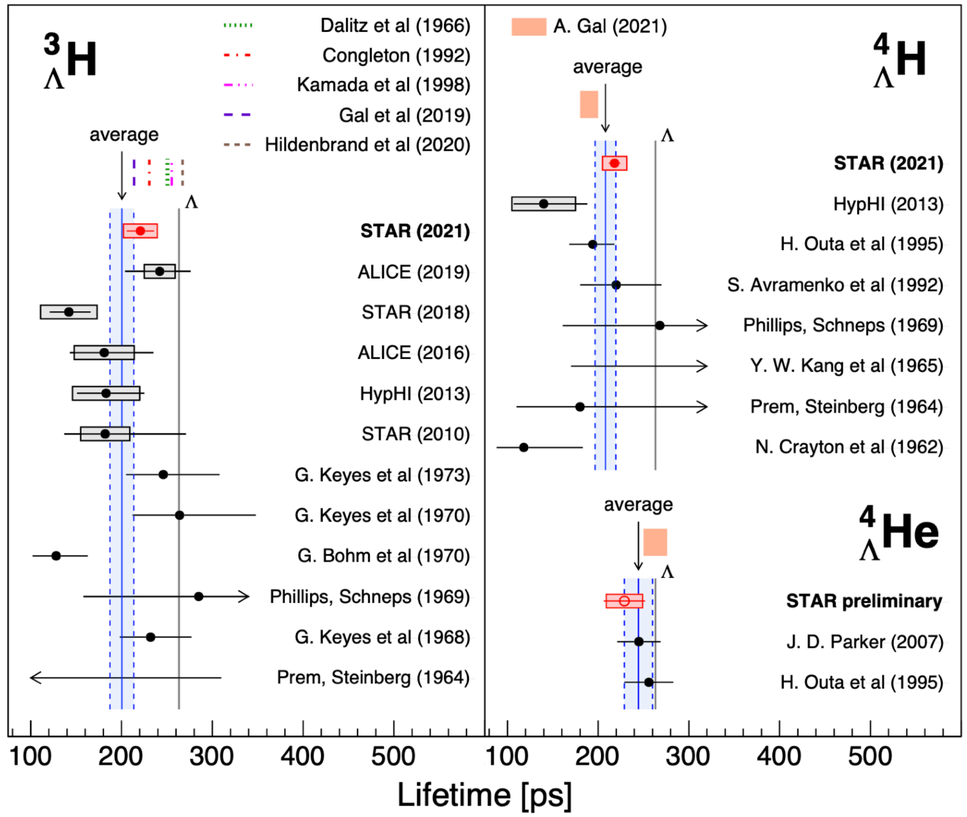

Hypernuclei $^3_\Lambda$H, ($^4_\Lambda$H) are reconstructed via 2 and 3 body decays ^{3}He + π and p + d + π , (^{4}He + π)